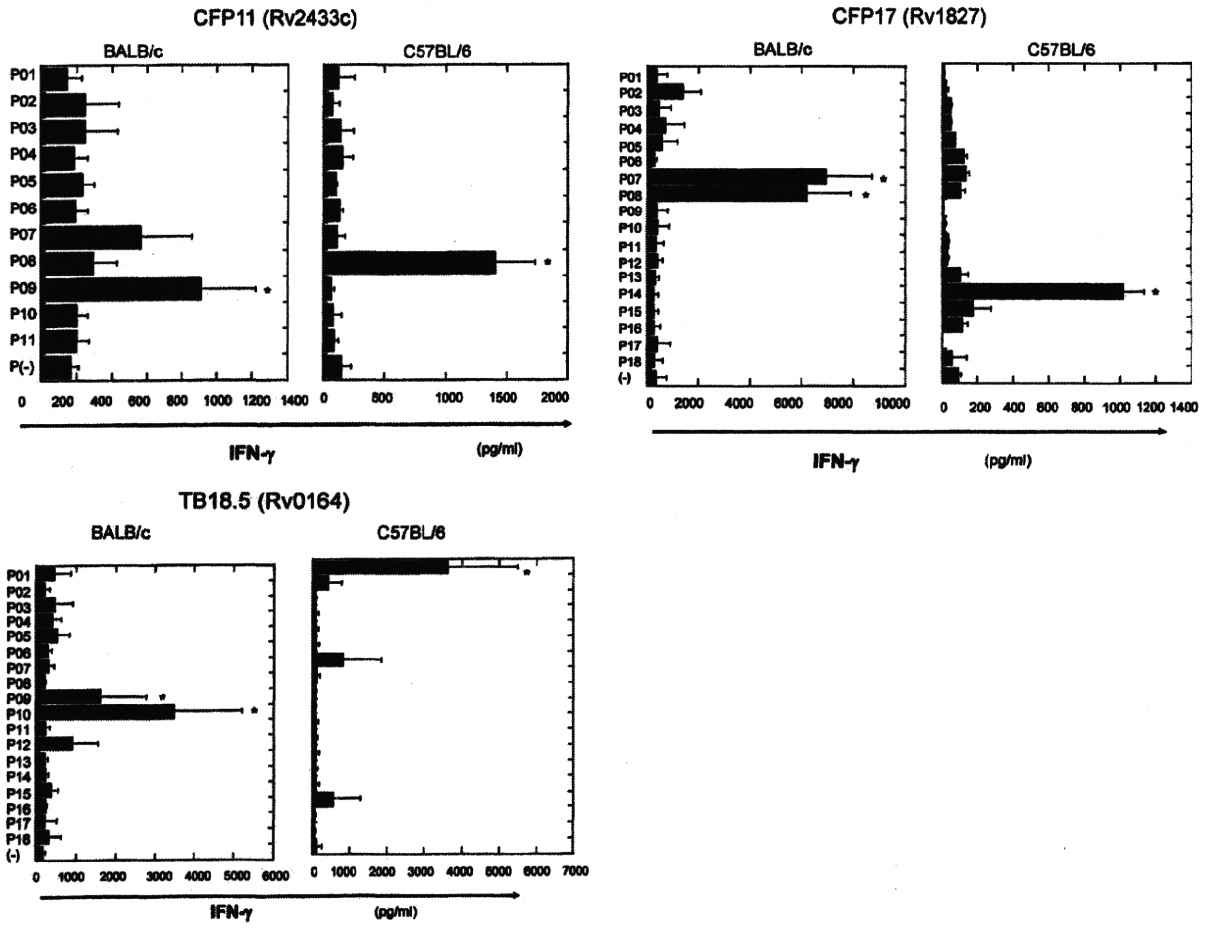

Fig. 2. IFN-γ production by splenocytes stimulated with overlapping peptides of CFP11, CFP17, and TB18.5 proteins. Inbred mice (BALB/c and C57BL/6) were immunized with plasmid DNA encoding CFP11, CFP17, or TB18.5 proteins using gene gun four times at 1-week intervals. The splenocytes were stimulated with overlapping peptides (7.5 μM) 2 weeks after the last immunization. IFN-γ amounts in the supernatants were analyzed by ELISA 72 h later. The means and SD from three mice are shown. Asterisks indicate statistical significance compared with the value without peptides ($P \leq 0.0001$).

2 μg of plasmid DNA and the injection was performed with a single shot of 0.5 mg gold cartridge (device helium discharge pressure: 400 lb/in.^{2}). Mice were injected with plasmid DNA four times at 1-week intervals.

2.4. Peptides

Peptides spanning the entire CFP11 (Rv2433c; 96 aa), CFP17 (Rv1827; 162 aa), and TB18.5 (Rv0164; 161 aa) aa sequences of *M. tuberculosis* were synthesized as approximately 20-mer peptides overlapping by 10 residues (Fig. 1) by Bio Synthesis (Lewisville, TX, USA). Short peptides used for minimal T-cell epitope determination were synthesized by Hayashi kasei (Osaka, Japan). All peptides were dissolved in phosphate-buffered saline (PBS) at a concentration of 1 mM and stored at −80 °C until use.

2.5. Prediction of T-cell epitopes by MHC binding peptide prediction algorithms

For the prediction of potential murine T-cell epitopes that could bind to MHC class I molecules, the following MHC binding peptide prediction algorithms were used through their web sites. These are the National Institutes of Health BioInformatics and Molecular Analysis Section (BIMAS) [31] (http://bimas.dcrt.nig.gov/cgi-bin/molbio/ken_parker_comboform), the SYFPEITHI program [32] (http://www.syfpeithi.de/), and the RANKPEP program [33] (http://bio.dfci.harvard.edu/Tools/rankpep.html).

2.6. Preparation of splenocyte culture supernatants

Two weeks after the last immunization, spleen cells were aseptically harvested from DNA-immune mice. A single cell suspension was prepared and red blood cells were lysed with ACK lysis solution (0.15 M NH_4Cl, 1 mM $KHCO_3$, and 0.1 mM EDTA, pH 7.2). Cells were cultured in RPMI 1640 medium supplemented with 10% heat-inactivated fetal calf serum (RPMI/10FCS) in 96-well plates at 1×10^6 cells (for BALB/c mice) or 2×10^6 cells (for C57BL/6 mice) per well in the presence or absence of 7.5 μM of each peptide at 37 °C in a 5% CO_2 atmosphere. Supernatants were harvested 72 h later and stored at −20 °C until they were assayed. The levels of IFN-γ in the culture supernatants were determined by a mouse-specific sandwich enzyme-linked immunosorbent assay (ELISA), as shown in our previous work [30].

2.7. Detection of IFNγ-producing cells by enzyme-linked immunospot (ELISPOT) assay

Single cell suspensions were tested for Ag-induced IFN-γ secretion using a standard cytokine BD ELISPOT system (BD Biosciences, San Jose, CA, USA). Briefly, cells were stimulated in RPMI/10FCS

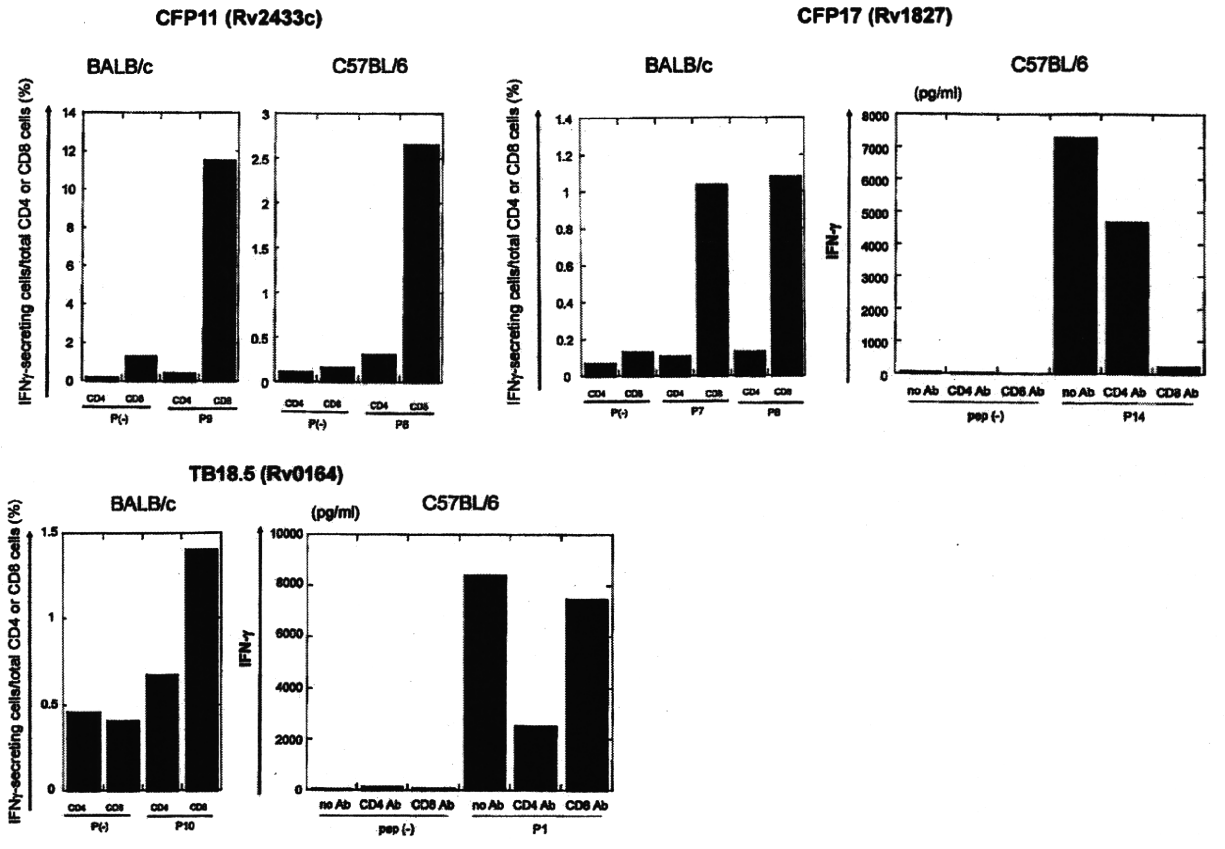

Fig. 3. Analysis of T-cell subsets responsive to CFP11, CFP17, and TB18.5 peptides. Mice were immunized with CFP11, CFP17, or TB18.5 DNA on the same schedule as in Fig. 2. Immune splenocytes were subjected to intracellular IFN-γ staining and cell-surface CD4/CD8 staining with respective mAbs. In the case of CFP17 and TB18.5 in C57BL/6, immune splenocytes were treated with magnetic beads specific for CD4 or CD8. Cells of the negative fraction were stimulated with respective peptides (7.5 μM). IFN-γ amounts in the supernatants were analyzed by ELISA 72 h later. The representative data from two to six mice are shown.

medium with 7.5 μM of each peptide in nitrocellulose-backed 96-well plates (MultiScreen 96-well plates; Millipore, Billerica, MA, USA) coated with 2.5 μg ml^{-1} anti-murine IFN-γ monoclonal antibody (mAb) (R4-6A2; BD Biosciences). The plates were incubated at 37 °C in a 5% CO_2 humidified incubator for 18–24 h. IFN-γ was detected by incubation with 0.75 μM of biotin-labeled anti-murine IFN-γ mAb XMG1.2 (BD Biosciences) for 2 h at room temperature followed by binding to horseradish peroxidase-conjugated streptavidin (eBioscience, San Diego, CA, USA). BD AEC (3-amino-9-ethyl-carbazole) substrate reagent (BD Biosciences) was used to detect bound horseradish peroxidase-conjugated streptavidin. Spots developed on the nitrocellulose filters were enumerated manually under a dissecting microscope.

2.8. Intracellular IFN-γ staining

The intracellular IFN-γ staining procedure was described in our previous work [30]. In brief, immune splenocytes were treated with ACK lysis solution to remove red blood cells, washed twice with RPMI 1640 medium and resuspended in RPMI/10FCS at a concentration of 10^7 cells ml^{-1}. The cells (200 μl) were incubated for 2 h at 37 °C in the presence or absence of 7.5 μM peptide. Golgistop solution (BD Biosciences) was added, further, the cells were incubated for an additional 4 h and then washed twice with FACS buffer (PBS supplemented with 1% FCS), stained with fluorescein isothiocyanate-conjugated anti-CD8 and PerCP-Cy5.5-conjugated anti-CD4 mAbs (BD Biosciences) on ice for 30 min and washed twice. Subsequently, intracellular IFN-γ staining was performed with phycoerythrin-conjugated anti-IFN-γ mAb (clone XMG1.2, BD Biosciences) using a Cytofix/Cytoperm kit (BD Biosciences) according to the manufacturer's instructions. These were analyzed with an EPICS digital flow cytometer (EPICS XL: Beckman Coulter, Miami, FL, USA).

2.9. Depletion of the CD4+ or CD8+ T-cell subset

CD4+ or CD8+ T-cell subsets of peptide-reactive T cells were examined by depletion of CD4+ or CD8+ T cells, respectively, using a BD IMag system (BD Biosciences). Briefly, immune splenocytes were resuspended and centrifuged at 1200 rpm with 1× BD IMag buffer. The supernatants were then carefully aspirated and 50 μl of anti-mouse CD4 particles-DM or anti-mouse CD8a particles-DM (BD Biosciences) was added for every 10^7 cells and the mixture was placed at 12 °C for 30 min. The labeled cells were adjusted to 5×10^7 cells ml^{-1} with 1× BD IMag buffer and immediately placed on BD IMagnet and incubated at room temperature for 8 min. The supernatants were carefully aspirated and confirmed to contain the fraction with either CD4+ or CD8+ T cells depleted by flow cytometry using fluorescent anti-CD4 or CD8 mAbs (data not shown).

2.10. MHC stabilization assay

MHC stabilization assay was originally described by Ljunggren and Kärre [34]. Wild-type RMA-S cells [35], or transfected RMAS-K^d, RMAS-D^d, or RMAS-L^d cells [30], were cultured in RPMI/10FCS at 26 °C overnight and then incubated for 1 h in the presence or

Table 1
T-cell epitope candidates in CFP11, CFP17, and TB18.5.

T-cell epitope candidates in CFP11, CFP17, and TB18.5				
Peptide	Amino acid sequence	Estimated scores for restriction molecules[a]		
CFP11 (BALB/c)		K^d	D^d	L^d
p69-86 (P9)	PFLVASVGYLGARRGVRR			
p76-84 (9mer)	GYLGARRGV	**1000** 24 17.9	—[b]	**2.0**
p70-78 (9mer)	FLVASVGYL	**115.2** 16	**1.2**	**5.0** 13
CFP11 (C57BL/6)		K^b	D^b	
p60-78 (P8)	VRMVINYLVPFLVASVGY			
p64-71 (8mer)	INYLVPFL	**6.6** 18 10.7	—	—
p61-69 (9mer)	RMVINYLVP	**0.2**	**3.9** 13	—
CFP17 (BALB/c)		K^d	D^d	L^d
p52-70 (P7)	PPGSALLVVKRGPNAGSRF			
p61-79 (P8)	KRGPNAGSRFLLDQAITSA			
p62-70 (9mer)	RGPNAGSRF	5	**120** 20.8	**15** 12
p62-69 (8mer)	RGPNAGSR	—	**4**	—
p63-71 (9mer)	GPNAGSRFL	**57.6** 9	**1**	**195** 23
CFP17 (C57BL/6)		K^b	D^b	
p112-130 (P14)	DVGSLNGTYVNREPVDSAV			
p113-121 (9mer)	VGSLNGTYV	—	**14.3** 23	
p113-122 (10mer)	VGSLNGTYVN	—	13	
p116-123 (8mer)	LNGTYVNR	**0.38** 13	13	
p117-126 (10mer)	NGTYVNREPV	—	**14.3**	
p118-126 (9mer)	GTYVNREPV	—	**12** 12.9	
TB18.5 (BALB/c)		K^d	D^d	L^d
p82-100 (P10)	AVYYPGENQIQTVMQQGEL			
p83-91 (9mer)	VYYPGENQI	**3456** 23 19.5	—	—
p84-91 (8mer)	YYPGENQI	**2000** 14.1	—	—

Epitopes predicted by computer algorithms are shown.
[a]Estimated scores are derived from BIMAS (bold), SYFPEITHI (underlined), or RANKPEP (plain).
[b]—; score not shown in the program.

absence of 50 μM of the respective peptides at 26 °C. The cells were then transferred to 37 °C for 2 h, washed with FACS buffer, and cell-surface expression of H2-K^b, H2-D^b, H2-K^d, H2-D^d, or H2-L^d molecules was detected by flow cytometry using FITC-conjugated mouse mAbs specific for H2-D^bL^d (28-14-8; eBioscience), H2-K^dD^d (34-1-2S; eBioscience), or H2-K^b (9013F; Cedarlane, Hornby, Ontario, Canada). To allow comparison between multiple experiments and to reduce interexperimental variations, the mean fluorescence intensity (MFI) values, which are direct measures of peptide binding, were converted to percent maximal stabilization values. The values were calculated using the following formula: (experimental MFI – control MFI)/(maximal MFI – control MFI) × 100. Control MFI was obtained from cells incubated without peptide at 37 °C while MFI of cells at 26 °C was taken as the maximal MFI.

2.11. Statistics

Statistical analyses were performed using the StatView-J 5.0 program (Abacus Concepts, Berkeley, CA, USA). Data from multiple experiments were expressed as mean and SD. Data were analyzed by analysis of variance (ANOVA) followed by a post-hoc Fisher protected least significant difference (PLSD) test.

3. Results

3.1. IFN-γ production by splenocytes of immune mice in response to overlapping synthetic peptides from CFP11 (Rv2433c), CFP17 (Rv1827), and TB18.5 (Rv0164)

Splenocytes of mice immunized with plasmid DNAs encoding CFP11, CFP17, or TB18.5 (pCI-CFP11, pCI-CFP17, or pCI-TB18.5, respectively) were stimulated with the overlapping peptides of the corresponding protein for 72 h and the IFN-γ concentration of the culture supernatants was measured by ELISA. As shown in Fig. 2, robust IFN-γ production was observed in splenocytes from the immune BALB/c mice (H2^d haplotype) in response to peptides P9 (aa 69–86), P7 (aa 52–70)/P8 (aa 61–79), or P9 (aa 72–89)/P10 (aa 82–100) for CFP11, CFP17, or TB18.5, respectively. Similarly, significantly high IFN-γ production was observed in splenocytes of the immune C57BL/6 mice (H2^b haplotype) in the presence of peptides

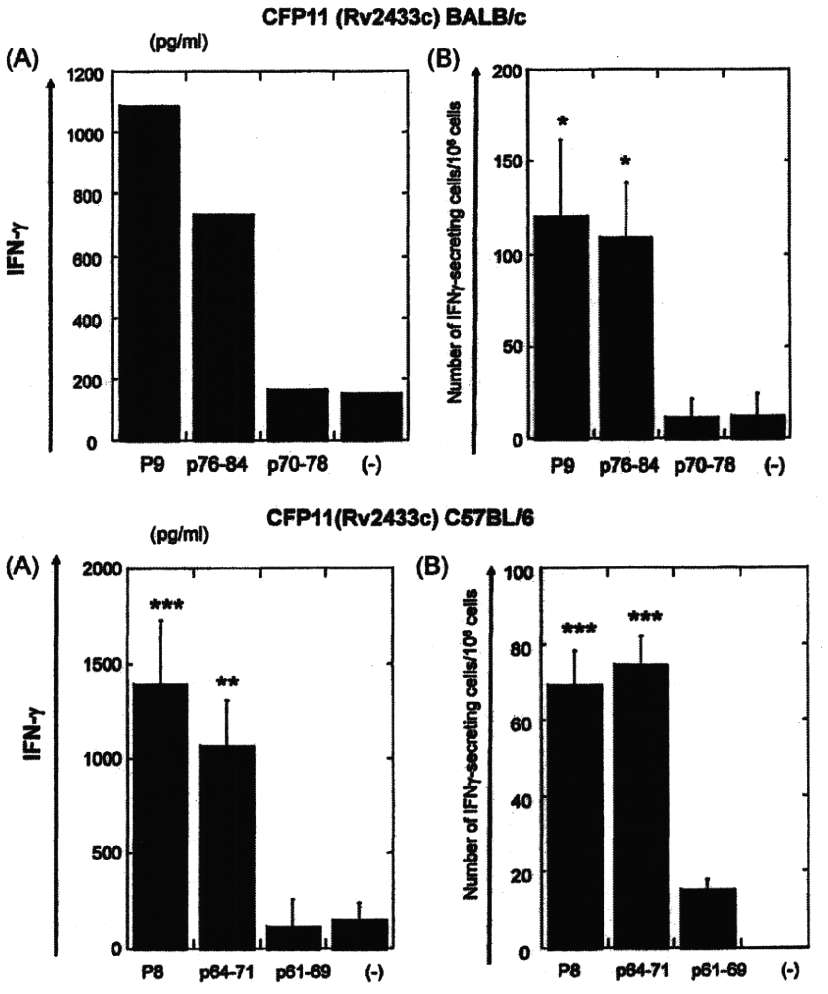

Fig. 4. Determination of minimal T-cell epitopes in CFP11 (Rv2433c) with ELISA and ELISPOT analyses. Inbred mice (BALB/c and C57BL/6) were immunized with CFP11 DNA on the same schedule as in Fig. 2. Immune splenocytes were stimulated with respective peptides (7.5 μM). IFN-γ amounts in the supernatants were analyzed by ELISA 72 h later, whereas the number of IFN-γ-producing cells was examined using ELISPOT 18-24 h later. The results of ELISA (A) and ELISPOT (B) are shown. The means ± SD from three mice are shown except for BALB/c ELISA, for which, the mean of two mice are shown. Asterisks indicate statistical significance compared with the value without peptides (***, $P \leq 0.0001$; **, $P \leq 0.001$; *, $P \leq 0.005$).

P8 (aa 61–77), P14 (aa 112–130), or P1 (aa 1–19) for CFP11, CFP17, or TB18.5, respectively.

3.2. Determination of T-cell subsets responsive to peptides of CFP11, CFP17, and TB18.5

Next, we examined the T-cell subsets that reacted to the peptides of CFP11, CFP17, and TB18.5. Intracellular IFN-γ staining analyses revealed that CD8+ T cells produced high amounts of IFN-γ in response to CFP11 P9 in BALB/c mice and P8 in C57BL/6 mice (Fig. 3). Similarly, CD8+ T cells produced high amounts of IFN-γ in response to CFP17 P7 and P8 peptides in BALB/c mice (Fig. 3). In TB18.5 DNA-immune BALB/c mice, CD8+ T cells produced high amounts of IFN-γ in response to TB18.5 P10 peptide (Fig. 3). In CFP17 and TB18.5 DNA-immune C57BL/6 mice, results of intracellular IFN-γ staining assays were not clear. Therefore, a CD4/CD8 depletion assay was performed. In the assay, CD4+ or CD8+ T cells were removed with magnetic beads and residual cells were stimulated with the relevant peptide. In the case of CFP17 DNA-immune C57BL/6 mice, treatment with CD8 mAb significantly reduced IFN-γ amounts in the culture supernatants whereas treatment of CD4 mAb did not affect the IFN-γ amounts, indicating that CD8+ T cells are the main producer of IFN-γ in the presence of CFP17 P14 peptide in C57BL/6 mice. In the case of TB18.5 DNA-immune C57BL/6 mice, treatment with CD4 mAb significantly reduced IFN-γ amounts in the culture supernatants whereas treatment of CD8 mAb did not affect the IFN-γ amounts, indicating that CD4+ T cells are the main producers of IFN-γ in the presence of TB18.5 P1 peptide in C57BL/6 mice (Fig. 3).

3.3. Identification of minimal T-cell epitopes in the responsive peptide regions of CFP11, CFP17, and TB18.5

Generally, CD8+ T cells recognize peptides of 8–11 aa residues on MHC class I molecules and CD4+ T cells recognize peptides of 12–18 aa residues on MHC class II molecules [36]. Several MHC binding peptide prediction algorithms are available on the Internet. We employed the BIMAS, SYFPEITHI, and RANKPEP programs for predicting CD8+ T-cell epitopes. Results of the analyses using these algorithms are summarized in Table 1.

In the CFP11 antigen, the p76-84 9-mer peptide (GYLGARRGV) in the P9 region showed the highest score (1000) for H2-K^d binding in the BIMAS program. Therefore, we examined the p76-84 peptide for induction of IFN-γ production using ELISA (Fig. 4). The

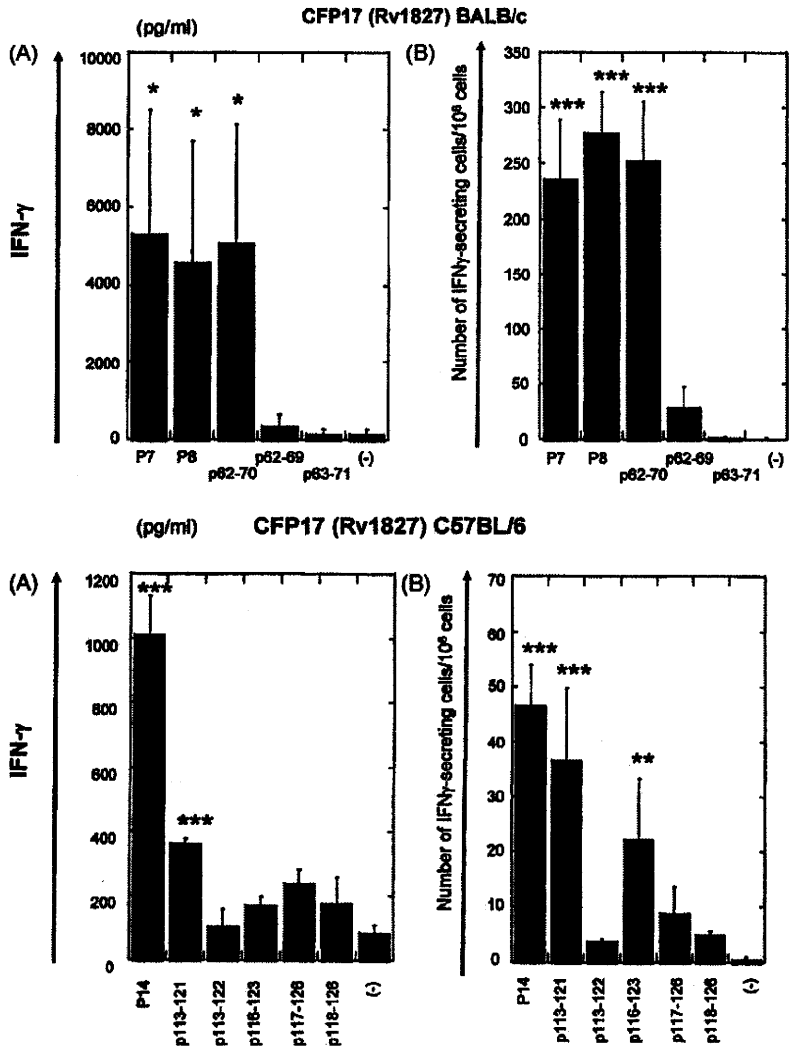

Fig. 5. Determination of minimal T-cell epitopes in CFP17 (Rv1827) with ELISA and ELISPOT analyses. Inbred mice (BALB/c and C57BL/6) were immunized with CFP17 DNA on the same schedule as in Fig. 2. ELISA and ELISPOT were performed as in Fig. 4 and the results of ELISA (A) and ELISPOT (B) are shown. The means and SD from three mice are shown. Asterisks indicate statistical significance compared with the value without peptides (***, $P \leq 0.0001$; **, $P \leq 0.005$; *, $P \leq 0.05$).

peptide induced robust IFN-γ production compared with the p70-78 peptide, which indicates that the p76-84 peptide is a minimal T-cell epitope. We detected a significantly high number of IFN-γ-secreting cells in immune splenocytes in the presence of P9 or the p76-84 peptide in ELISPOT assay (Fig. 4). In C57BL/6 mice, the algorithms gave the highest score for binding to H2-K^b to the p64-71 peptide (INYLVPFL; Table 1). The p64-71 peptide stimulation showed significantly high IFN-γ levels on ELISA and significantly high IFN-γ-producing cell numbers on ELISPOT assay (Fig. 4).

In the CFP17 antigen, the p62-70 9-mer peptide (RGPNAGSRF) in the P7/P8 region showed high scores (120 in BIMAS; 20.8 in RANKPEP) for H2-D^d binding (Table 1). Therefore, we examined the p62-70 peptide for induction of IFN-γ production using ELISA and ELISPOT assays. The p62-70 peptide stimulation showed significantly high IFN-γ amounts on ELISA and significantly high numbers of IFN-γ-producing cells on ELISPOT assay (Fig. 5), indicating that the p62-70 peptide is a minimal T-cell epitope. In C57BL/6 mice, SYFPEITHI algorithm gave a high score for binding to H2-D^b to the p113-121 peptide (VGSLNGTYV; Table 1), and the peptide showed significantly high levels of IFN-γ production and significantly high numbers of IFN-γ-producing cells with ELISA and ELISPOT assays, respectively (Fig. 5).

In the TB18.5 antigen, the p83-91 9-mer peptide (VYYPGENQI) in the P10 region has a high score (3456) for H2-K^d binding in the BIMAS program (Table 1). Therefore, we examined the p83-91 peptide for induction of IFN-γ production using ELISA and determined the number of IFN-γ-producing cells via ELISPOT assay. The p83-91 peptide induced robust IFN-γ production compared with p84-91, which indicates that the p83-91 peptide is a minimal T-cell epitope (Fig. 6). In C57BL/6 mice, no peptides were predicted to bind to K^b or D^b with high scores, although P1 of TB18.5 elicited robust IFN-γ production (Fig. 2) and CD4+ T cells were the main IFN-γ producer (Fig. 3). Since C57BL/6 mice have a deletion of the H2-Eα gene, therefore, they do not express H2-E molecules on the cell surface [37], the identified CD4+ T-cell epitopes in C57BL/6 mice are considered to be exclusively presented on H2-A^b.

3.4. Identification of MHC class I restriction molecules for CFP11, CFP17, and TB18.5 minimal epitopes

Finally, we investigated the binding and stabilization of MHC class I restriction molecules by each identified minimal epitope of CFP11, CFP17, or TB18.5. As shown in Fig. 7, the p76-84 peptide of CFP11 and p83-91 of TB18.5 were strongly bound to the H2-K^d

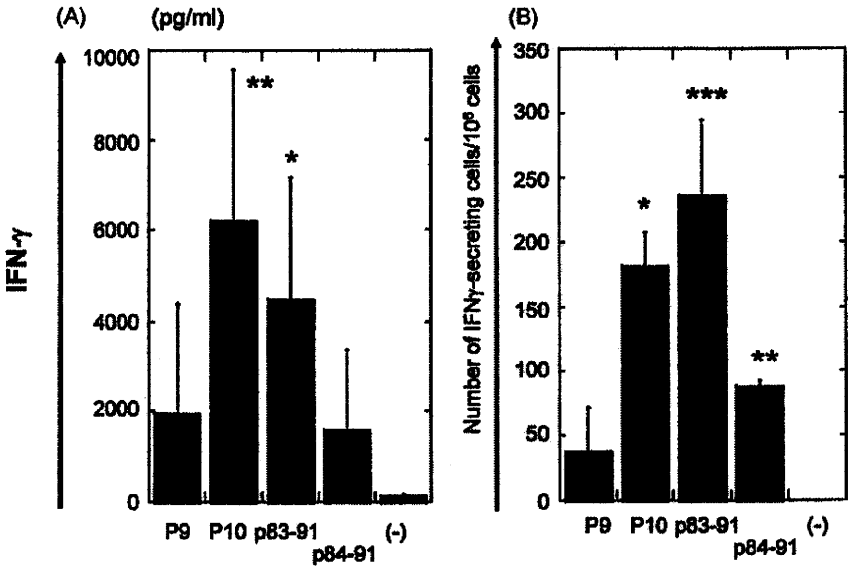

Fig. 6. Determination of minimal T-cell epitopes in TB18.5 (Rv0164) with ELISA and ELISPOT analyses. BALB/c mice were immunized with TB18.5 DNA on the same schedule as in Fig. 2. ELISA and ELISPOT were performed as in Fig. 4 and the results of ELISA (A) and ELISPOT (B) are shown. The means and SD from three mice are shown. Asterisks indicate statistical significance compared with the value without peptides (***, $P \leq 0.0001$; **, $P \leq 0.01$; *, $P \leq 0.05$).

molecule, whereas p62-70 of CFP17 was strongly bound to the H2-D^d molecule. In addition, p64-71 of CFP11 was bound to H2-K^b and p113-121 of CFP17 was bound to the H2-D^b molecule.

4. Discussion

T cells have several features that are important for protective immunity against *M. tuberculosis*. These include production of proinflammatory cytokines such as IFN-γ and tumor necrosis factor-α. IFN-γ has been regarded as an important correlate of protective immune responses [38]. Activation of macrophages harboring *M. tuberculosis* by IFN-γ has been considered to be crucial for eradication of the intracellular bacterium. In addition, the majority of IFN-γ-producing CD8+ T cells have cytotoxic activity for cells harboring the bacterium, which also contribute to protective ability. Analyses of the protective ability of the CD8+ T-cell epitope peptides identified in this study is required to clarify their physiological functions.

We have performed ELISA and ELISPOT assays for the identification of minimal epitopes in this study. Basically, both ELISA and ELISPOT assays showed similar results. However, we noticed that in some cases these results differed. For example, P7 of CFP17 in BALB/c mice (Fig. 5) induced higher IFN-γ production than P8 on ELISA, but P8 induced a higher number of IFN-γ-producing cells than P7 on ELISPOT assay. Although the differences were not very high, similar results were obtained each time we performed the experiments. The difference in the additional flanking aa residues next to the common minimal epitope aa sequence in the peptides may affect the stability of peptides and the kinetics of IFN-γ production during the different incubation times of ELISA (72 h) and ELISPOT (18–24 h). This may account for the differences observed between the ELISA and ELISPOT results.

The T-cell epitopes identified in this study were all CD8+ T-cell epitopes except for one CD4+ T-cell epitope in the TB18.5 protein in C57BL/6 mice. This may be caused in part by the fact that DNA immunization is an efficient method for producing cytoplasmic antigens that are consequently detected by CD8+ T cells. In addition, low-molecular-mass proteins may be easily degraded to smaller peptides that tend to be subject to the antigen presentation pathway through MHC class Ia molecules. Of note, among mouse MHC binding motifs, the H2-K^d binding motifs have been shown to be quite similar to those of HLA-A24 [39], which is the most popular subtype of HLA-A (approximately 60%) of the Japanese population [40]. Therefore, the H2-K^d-restricted T-cell epitopes identified in this study may also function as HLA-A24-restricted epitopes although further investigation is needed to confirm this.

The T-cell epitope repertoire determined by DNA immunization method, using plasmids encoding mycobacterial antigens has been reported to be broader than that stimulated by live mycobacterial infection. A variety of peptides induced IFN-γ and/or IL-2 production in mice immunized with plasmid DNA encoding Ag85A, Ag85B, or Ag85C [27,28]. However, in our study, only one peptide or two overlapping peptides of CFP11, CFP17, or TB18.5 in BALB/c or C57BL/6 mouse strains induced IFN-γ production from immune splenocytes. This may be due to the small size of the proteins examined here compared with the Ag85 family proteins. Previously, we observed that only a restricted peptide region (one or two 20-mer peptides) induced IFN-γ production in mice immunized with DNA encoding MPT51 that has a molecular mass similar to that of the Ag85 family proteins [29,30]. In addition, our previous work [41] showed that only one immunodominant epitope of Ag85A was detected in the dendritic cell immunization system of BALB/c mice, although at least three epitope peptides have been reported [27]. The mechanism of optimum epitope selection from several predicted peptides that fit well with the MHC binding motifs remains to be clarified.

Concerning the importance of T-cell epitope mapping in mice, immunodominant antigens in mice are also generally immunodominant in humans. However, precise, specific T-cell analyses are possible only in mice. Therefore, T-cell epitope mapping in mice and analyses using the identified epitope peptides will provide important information that can be used for better understanding of T cells specific for antigens of *M. tuberculosis*, although T-cell epitope peptides themselves are, in principle, different between mice and humans. T-cell epitope mapping is critical for the accurate analysis of T cells specific for antigens and for the design of epitope-based vaccines [42,43].

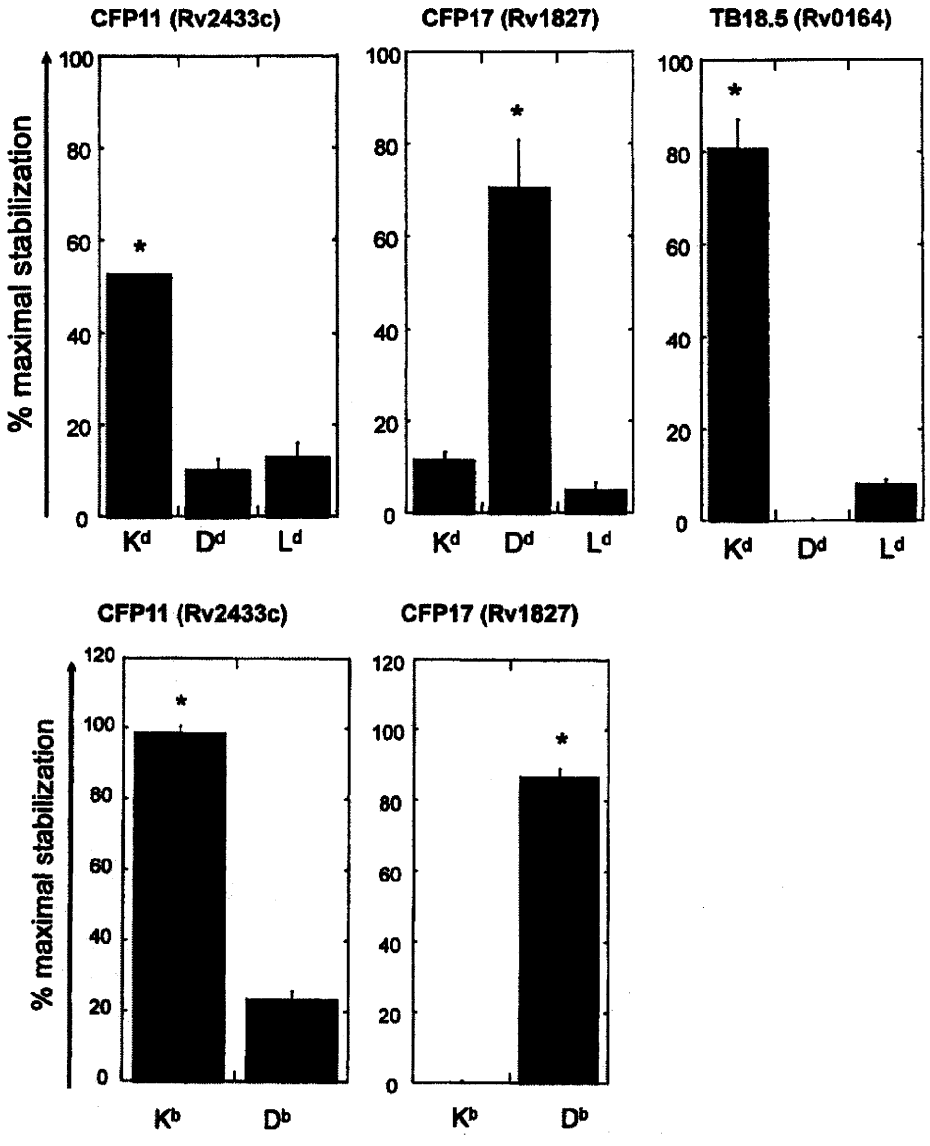

Fig. 7. MHC binding assay of peptides from CFP11, CFP17, and TB18.5. The ability of CD8+ T-cell epitope candidate peptides to bind to MHC class I molecules was measured by MHC stabilization assay using RMA-S cells (for H2-K^b and D^b molecules) or the transfectants, RMAS-K^d, RMAS-D^d, or RMAS-L^d cells (for H2-K^d, D^d, and L^d molecules, respectively). The results are expressed as percent maximal stabilization values and SD. Asterisks indicate statistical significance compared with the value without peptides ($P \leq 0.0001$).

In conclusion, we identified murine T-cell epitopes of CFP11, CFP17, and TB18.5, which are immunoreactive low-molecular-mass antigens of *M. tuberculosis*. We identified two CD8+ T-cell epitopes on CFP11 and CFP17, one in BALB/c mice and the other in C57BL/6 mice, respectively. On TB18.5, we identified a CD8+ T-cell epitope in BALB/c mice and a CD4+ T-cell epitope in C57BL/6 mice. With the aid of computer algorithms, we could identify the minimal CD8+ T-cell epitopes. T-cell epitopes of CFP11, CFP17, and TB18.5, as well as MPT51, would be feasible for analysis of T-cell responses to *M. tuberculosis* infection.

Acknowledgements

This work was supported by Grants-in-Aid for Scientific Research (grant nos. 20590438 to T.N., 20590439 to K.T., and 20390125 to Y.K.) from the Japanese Society for the Promotion of Science, a Grant-in-Aid for Scientific Research on Priority Areas (grant no. 17016089 to K.T.) from the Ministry of Education, Culture, Sports, Science and Technology of Japan, and by a Grant-in-Aid from the United States–Japan Cooperative Medical Science Program (Y.K.).

References

[1] World Health Organization. WHO Report 2009 Global tuberculosis control: epidemiology, strategy, financing. Geneva. http://www.who.int/tb/publications/global_report/2009/pdf/full_report.pdf; 2009 [online].
[2] Andersen P, Doherty TM. The success and failure of BCG — implications for a novel tuberculosis vaccine. Nat Rev Microbiol 2005;3:656–62.
[3] Bloom BR, Fine PEM. The BCG experience: implications for future vaccines against tuberculosis. In: Tuberculosis: pathogenesis, protection, and control. Washington, DC: ASM Press; 1994. p. 531–57.
[4] Fine PEM. Variation in protection by BCG: implications of and for heterologous immunity. Lancet 1995;346:1339–45.
[5] Sterne JAC, Rodrigues LC, Guedes IN. Does the efficacy of BCG decline with time since vaccination? Int J Tuberc Lung Dis 1998;2:200–7.

[6] Kaufmann SHE, Baumann S, Nasser Eddine A. Exploiting immunology and molecular genetics for rational vaccine design against tuberculosis. Int J Tuberc Lung Dis 2006;10:1068–79.
[7] Cooper AM. Cell-mediated immune responses in tuberculosis. Annu Rev Immunol 2009;27:393–422.
[8] Kaufmann SHE. How can immunology contribute to the control of tuberculosis? Nat Rev Immunol 2001;1:20–30.
[9] Smith SM, Duckrell HM. Role of CD8+ T cells in mycobacterial infections. Immunol Cell Biol 2000;78:325–33.
[10] Kaufumann SHE, Flynn JL. CD8 T cells in tuberculosis. In: Cole ST, Eisenach KD, McMurray DN, Jacobs Jr WR, editors. Tuberculosis and the tubercle bacillus. Washington, DC: ASM Press; 2005. p. 465–74.
[11] Sable SB, Karlra M, Verma I, Khuller GK. Tuberculosis subunit vaccine design: the conflict of antigenicity and immunogenicity. Clin Immunol 2007;122:239–51.
[12] Cole ST, Brosch R, Parkhill J, Garunier T, Churcher C, Harris D, et al. Deciphering the biology of *Mycobacterium tuberculosis* from the complete genome sequence. Nature 1998;393:537–44.
[13] Orme IA. Induction of nonspecific acquired resistance and delayed-type hypersensitivity, but not specific acquired resistance, in mice inoculated with killed mycobacterial vaccines. Infect Immun 1988;56:3310–2.
[14] Andersen P. Effective vaccination of mice against *Mycobacterium tuberculosis* infection with a soluble mixture of secreted mycobacterial proteins. Infect Immun 1994;62:2536–44.
[15] Horwitz MA, Lee BWE, Dillon BJ, Harth G. Protective immunity against tuberculosis induced by vaccination with major extracellular proteins of *Mycobacterium tuberculosis*. Proc Natl Acad Sci U S A 1995;92:1530–4.
[16] Roberts AD, Sonnenberg MG, Ordway DJ, Furney SK, Brennan PJ, Belisle JT, et al. Characteristics of protective immunity engendered by vaccination of mice with purified culture filtrate protein antigens of *Mycobacterium tuberculosis*. Immunology 1995;85:502–8.
[17] Boesen H, Jensen BN, Wilcke T, Andersen P. Human T-cell responses to secreted antigen fractions of *Mycobacterium tuberculosis*. Infect Immun 1995;63:1491–7.
[18] Demissie A, Ravn P, Olobo J, Doherty TM, Eguale T, Geletu M, et al. T-cell recognition of *Mycobacterium tuberculosis* culture filtrate fractions in tuberculosis patients and their household contacts. Infect Immun 1999;67:5967–71.
[19] Andersen P, Munk ME, Pollock JM, Doherty TM. Specific immune-based diagnosis of tuberculosis. Lancet 2000;356:1099–104.
[20] Weldingh K, Rosenkrands I, Jacobsen S, Rasmussen PB, Elhay MJ, Andersen P. Two-dimensional electrophoresis for analysis of *Mycobacterium tuberculosis* culture filtrate and purification and characterization of six novel proteins. Infect Immun 1998;66:3492–500.
[21] Weldingh K, Andersen P. Immunological evaluation of novel *Mycobacterium tuberculosis* culture filtrate proteins. FEMS Immunol Med Microbiol 1999;23:159–64.
[22] Lim JH, Kim HJ, Lee KS, Jo EK, Song CH, Jung SB, et al. Identification of the new T-cell-stimulating antigens from *Mycobacterium tuberculosis* culture filtrate. FEMS Microbiol Lett 2004;232:51–9.
[23] Sable SB, Kumar R, Kalra M, Verma I, Khuller GK, Dobos K, et al. Peripheral blood and pleural fluid mononuclear cell responses to low-molecular-mass secretory polypeptides of *Mycobacterium tuberculosis* in human models of immunity to tuberculosis. Infect Immun 2005;73:3547–58.
[24] Belisle JT, Braunstein M, Rosenkrands I, Andersen P. The proteome of *Mycobacterium tuberculosis*. In: Cole ST, Eisenach KD, McMurray DN, Jacobs Jr WR, editors. Tuberculosis and the tubercle bacillus. Washington, DC: ASM Press; 2005. p. 235–60.
[25] Bu L, Brooks III CL. De novo prediction of the structures of *M. Tuberculosis* membrane proteins. J Am Chem Soc 2008;130:5384–5.
[26] Yoshida A, Nagata T, Uchijima M, Higashi T, Koide Y. Advantage of gene gun-mediated over intramuscular inoculation of plasmid DNA vaccine in reproducible induction of specific immune responses. Vaccine 2000;18:1725–9.
[27] Denis O, Tanghe A, Palfliet K, Jurion F, van den Berg T, Vanonckelen A, et al. Vaccination with plasmid DNA encoding mycobacterial antigen 85A stimulates a CD4+ and CD8+ T-cell epitopic repertoire broader than that stimulated by *Mycobacterium tuberculosis* H37Rv infection. Infect Immun 1998;66:1527–33.
[28] D'Souza S, Rosseels V, Romano M, Tanghe A, Denis O, Jurion F, et al. Mapping of murine Th1 helper T-cell epitopes of mycolyl transferases Ag85A, Ag85B, and Ag85C from *Mycobacterium tuberculosis*. Infect Immun 2003;71:483–93.
[29] Aoshi T, Nagata T, Suzuki M, Uchijima M, Hashimoto D, Rafiei A, et al. Identification of an HLA-A*0201-restricted T-cell epitope on MPT51 protein, a major secreted protein derived from *Mycobacterium tuberculosis* by MPT51 overlapping peptide screening. Infect Immun 2008;76:1565–71.
[30] Suzuki M, Aoshi T, Nagata T, Koide Y. Identification of murine H2-D^d- and H2-A^b-restricted T-cell epitopes on a novel protective antigen, MPT51, of *Mycobacterium tuberculosis*. Infect Immun 2004;72:3829–37.
[31] Parker KC, Bednarek MA, Coligan JE. Scheme for ranking potential HLA-A2 binding peptides based on independent binding of individual peptide side-chains. J Immunol 1994;152:163–75.
[32] Rammensee H-G, Bachmann J, Emmerich NPN, Bachor OA, Sevanović S. SYFPEITHI: database for MHC ligands and peptide motifs. Immunogenetics 1999;50:213–9.
[33] Reche PA, Glutting J-P, Zhang H, Reinherz EL. Enhancement to the RANKPEP resource for the prediction of peptide binding to MHC molecules using profiles. Immunogenetics 2004;56:405–19.
[34] Ljunggren H-G, Kärre K. Host resistance directed selectively against H-2-deficient lymphoma variants. J Exp Med 1985;162:1745–59.
[35] Ljunggren H-G, Stam NJ, Öhlén C, Neefjes JJ, Höglund P, Heemels M-T, et al. Empty MHC class I molecules come out in the cold. Nature 1990;346:476–80.
[36] Margulies DH, Natarajan K, Rossjohn J, McClusky J. Major histocompatibility complex (MHC) molecules: structure, function, and genetics. In: Paul WE, editor. Fundamental immunology. 6th ed. Philadelphia: Lippincott Williams & Wilkins Publishers; 2008. p. 570–613.
[37] Mathis DJ, Benoist C, Williams II VE, Kanter M, McDevitt HO. Several mechanisms can account for defective $E\alpha$ gene expression in different mouse haplotypes. Proc Natl Acad Sci U S A 1983;80:273–7.
[38] Ellner JJ, Hirsch CS, Whalen CC. Correlates of protective immunity to *Mycobacterium tuberculosis* in humans. Clin Infect Dis 2000;30(Suppl. 3):S279–82.
[39] Okunaga T, Ikuta Y, Takahashi Y, Obata H, Tanida K, Watanabe M, et al. A novel human HER2-derived peptide homologous to the mouse K^d-restricted tumor rejection antigen can induce HLA-A24-restricted cytotoxic T lymphocytes in ovarian cancer patients and healthy individuals. Eur J Immunol 2000;30:3338–46.
[40] Date Y, Kimura A, Kato H, Sasazuki T. DNA typing of the HLA-A gene: population study and identification of four new alleles in Japanese. Tissue Antigens 1996;47:93–101.
[41] Nakano H, Nagata T, Suda T, Tanaka T, Aoshi T, Uchijima M, et al. Immunization with dendritic cells retrovirally transduced with mycobacterial antigen 85A gene elicits the specific cellular immunity including cytotoxic T-lymphocyte activity specific to an epitope on antigen 85A. Infect Immun 2006;24:2110–9.
[42] Fonseca DPAJ, Benaissa-Trouw B, van Engelen M, Kraaijeveld CA, Snippe H, Verheul AFM. Induction of cell-mediated immunity against *Mycobacterium tuberculosis* using DNA vaccines encoding cytotoxic and helper T-cell epitopes of the 38-kilodalton protein. Infect Immun 2001;69:4839–45.
[43] Gao H, Yue Y, Hu L, Xu W, Xiong S. A novel DNA vaccine containing multiple TB-specific epitopes casted in a natural structure (ECANS) confers protective immunity against pulmonary mycobacterial challenge. Vaccine 2009;27:5313–9.

Microbiology and Immunology

Microbiol Immunol 2010; 54: 170–174
doi:10.1111/j.1348-0421.2009.00199.x

NOTE

Differential recruitment of CD63 and Rab7-interacting-lysosomal-protein to phagosomes containing *Mycobacterium tuberculosis* in macrophages

Shintaro Seto[1], Sohkichi Matsumoto[2], Kunio Tsujimura[1] and Yukio Koide[1]

[1]Department of Infectious Diseases, Hamamatsu University School of Medicine, 1-20-1 Handayama, Higashi-ku, Hamamatsu, 431-3192, and [2]Department of Bacteriology, Osaka City University Graduate School of Medicine, 1-4-3, Asahi-machi, Abeno-ku, Osaka 545-8585, Japan

ABSTRACT

***M.tb* is an intracellular pathogen which survives within the phagosomes of host macrophages by inhibiting their fusion with lysosomes. Here, it has been demonstrated that a lysosomal glycoprotein, CD63, is recruited to the majority of *M.tb* phagosomes, while RILP shows limited localization. This is consistent with the author's findings that CD63, but not RILP, is recruited to the phagosomes in macrophages expressing the dominant negative form of Rab7. These results suggest that *M.tb* phagosomes selectively fuse with endosomes and lysosomes to escape killing activity while acquiring nutrients.**

Key words lysosome, macrophage, *Mycobacterium tuberculosis*, phagosome.

Phagocytosis of infected pathogens by macrophages plays an important role in the early stages of innate immunity. Phagocytosed pathogens are incorporated into phagosomal vacuoles. These phagosomes then interact with endosomal and lysosomal vesicles in a process referred to as phagolysosome biogenesis. During phagolysosome biogenesis, phagosomes acquire degradative and microbicidal properties, leading phagocytosed pathogens to be killed and degraded.

M.tb, the causative bacterium of tuberculosis, infects more than one-third of the human population. *M.tb* is able to survive and proliferate within phagosomes of the host's macrophages by inhibiting phagolysosome biogenesis (1, 2). However, the exact process by which *M.tb* blocks phagolysosome biogenesis is not fully understood. Recently, it was reported that phagosomes containing *M.tb* (*M.tb* phagosomes) within dendritic cells are associated with lysosomes in the early stages of infection (3). In addition, we have previously demonstrated that LAMP-2, but not cathepsin D, is recruited to *M.tb* phagosomes in macrophages (4). These results suggest that *M.tb* phagosomes selectively fuse with lysosomal vesicles which have distinct characteristics. To investigate this possibility, we further examined the localization of two lysosomal marker proteins, CD63 and RILP, on *M.tb* phagosomes in this study.

Raw264.7 macrophage was obtained from the American Type Culture Collection (Manassas, VA, USA) and maintained in Dulbecco's modified Eagle's medium supplemented with 10% FBS (Invitrogen, Carlsbad, CA, USA), 25 μg/ml penicillin G, and 25 μg/ml streptomycin at 37°C in 5% CO_2. *M.tb* strain H37Rv and *Mycobacterium smegmatis* mc^2155 were grown in 7H9 medium supplemented with 10% Middlebrook ADC (BD Biosciences, San Jose, CA, USA), 0.5% glycerol, 0.05% Tween 80 (mycobacteria complete medium) at 37°C. *M tb* strain H37Rv transformed with a plasmid encoding DsRed (5) was grown in mycobacteria complete medium with 25 μg/ml kanamycin at 37°C. To construct the plasmids encoding CD63-EGFP and EGFP-RILP, PCR

Correspondence
Yukio Koide, Executive Director, Hamamatsu University School of Medicine, 1-20-1 Handayama, Higashi-ku, Hamamatsu, 431-3192, Japan.
Tel: +81 53 435 2101; fax: +81 53 435 2101; email: koidelb@hama-med.ac.jp

Received 27 October 2009; revised 18 November 2009; accepted 20 November 2009.

List of Abbreviations: CLSM, confocal laser scanning microscopy; LAMP-2, lysosomal associated membrane protein-2; *M. smegmatis*, *Mycobacterium smegmatis*; *M.tb*, *Mycobacterium tuberculosis*; MTOC, microtubule-organizing center; RILP, Rab7-interacting-lysosomal-proteins.

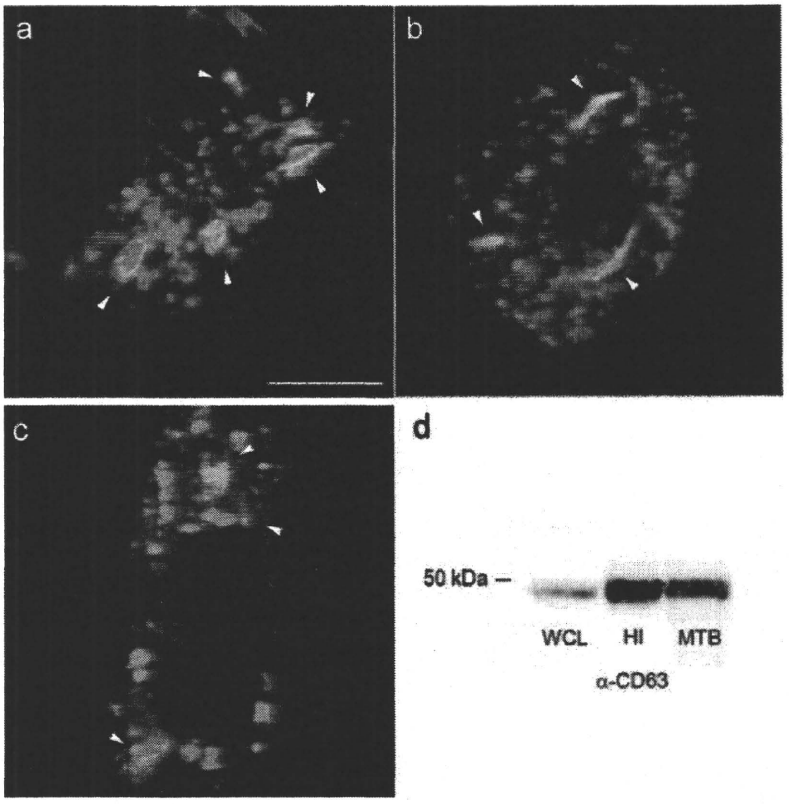

Fig. 1. Localization of CD63 on *M.tb* phagosomes. (a, b) Raw264.7 macrophages expressing CD63-EGFP were infected with *M.tb* expressing DsRed for (a) 30 min and (b) 6 hr. Infected cells were fixed and observed by CLSM. (c) *M.tb*-infected Raw264.7 macrophages were stained with anti-CD63 and Alexa488-conjugated anti-rat IgG antibodies and observed by CLSM. Arrowheads indicate CD63-positive phagosomes; scale bar, 10 μm. (d) CD63 localization in isolated mycobacterial phagosome fractions. Whole cell lysates from Raw264.7, the heat-inactivated *M. smegmatis* phagosome and live *M.tb* phagosome fractions were subjected to SDS-PAGE, followed by immunoblotting using anti-CD63 antibody. HI, heat-inactivated *M. smegmatis* phagosome fraction; MTB, live *M.tb* phagosome fraction; WCL, Raw264.7.

was carried out using cDNA derived from HeLa cells as a template and the following primer sets: human CD63 (5′-CCTCGAGCCACCATGGCGGTGGAAGGAGGAATGAA ATG-3′ and 5′-CGGATCCCCATCACCTCGTAGCCACTT CTGATAC-3′), and human RILP (5′-CAGATCTATGGAG CCCAGGAGGGCGGC-3′ and 5′-CGAATTCTCAG GCCTCTGGGGCGGCTG-3′). The PCR products of CD63 and RILP were inserted into pEGFP-N2 and pEGFP-C1 vectors (Clontech, Mountain View, CA, USA), respectively. Transfection of macrophages with plasmids, infection of bacteria with transfected macrophages, CLSM, immunofluorescence microscopy, and isolation of mycobacterial phagosomes were performed as described previously (4). For immunofluorescence microscopy, macrophages were stained with rat anti-CD63 monoclonal antibody (1:30 v/v, MBL, Nagoya, Japan) and Alexa488-conjugated anti-rat IgG antibody (1:1000 v/v, Invitrogen). For immunoblotting analysis, aliquots of 40 μg of cell lysates from Raw264.7 and 15 μg of phagosomal fraction proteins were separated by SDS-PAGE and then subjected to immunoblotting analysis using rat anti-CD63 monoclonal antibody (1:100 v/v, MBL). The unpaired two-sided Student's *t*-test was used to assess the statistical significance of the differences between the two groups.

CD63 has been shown to be localized to the phagosome during phagolysosome biogenesis (2, 6), but its localization on live mycobacterial phagosomes is still controversial (2, 3, 7). CD63 was originally identified as a platelet activation marker (8) and has also been used as a marker for late endosomes and lysosomes because of its function in phagosome acidification (9–12). We therefore re-assessed CD63 localization on *M.tb* phagosomes in infected macrophages (Fig. 1). Raw264.7 macrophages transfected with a plasmid encoding CD63-EGFP were infected with *M.tb* expressing DsRed. Infected cells were fixed and observed by CLSM. Clear CD63 localization was observed on more than 60% of *M.tb* phagosomes at 30 min and 6 hr post infection (Fig. 1a, b). To rule out the possibility that CD63 localization on *M.tb* phagosomes is caused by exogenous expression of CD63-EGFP, immunofluorescence microscopy with anti-CD63 antibody was performed (Fig. 1c). We found that endogenous CD63 was also localized to about 60% of *M.tb* phagosomes at 6 hr post infection. To confirm the recruitment of CD63 to live *M.tb* phagosomes biochemically, we carried out

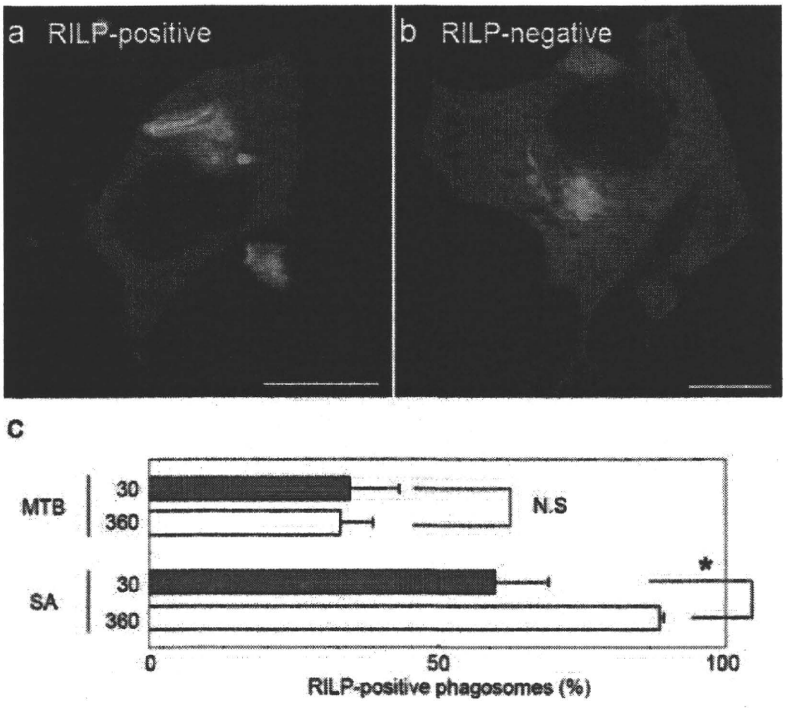

Fig. 2. Localization of RILP on *M.tb* phagosomes. (a, b) Raw264.7 macrophages expressing EGFP-RILP were infected with *M.tb* expressing DsRed. Infected cells were fixed and observed by CLSM. (a) and (b) show representative cell images of RILP-positive and RILP-negative *M.tb* phagosomes, respectively. Scale bar, 10 μm. (c) The proportion of RILP-positive phagosomes of *M.tb* and *Staphylococcus aureus* at 30 min and 360 min postinfection. *, $P < 0.05$; MTB, proportion of RILP-positive phagosomes of *M.tb;* N.S, no significant difference between the groups; SA, proportion of RILP-positive phagosomes of *Staphylococcus aureus.*

immunoblotting analysis for CD63 in isolated mycobacterial phagosome fractions (Fig. 1d). Raw264.7 macrophages were allowed to phagocytose heat-inactivated *M. smegmatis* or infected with *M.tb* for 6 hr, and the phagosomal fractions isolated as described previously (4, 13). Proteins extracted from isolated phagosomal fractions were subjected to immunoblotting analysis using anti-CD63 antibody. Immunoblotting analysis revealed that CD63 is recruited to live *M.tb* phagosomes as well as to heat-inactivated *M. smegmatis* phagosomes. These results suggest that *M.tb* phagosomes fuse with CD63-positive lysosomal vesicles.

RILP interacts with the active form of Rab7 and mediates the fusion of endosomes with lysosomes (14, 15). RILP is also reported to be localized to the phagosome and to recruit the minus-end motor complex dynein-dynactin to the phagosome, resulting in migration of the phagosome to the MTOC where late endosomal and lysosomal vesicles accumulate (16). In the process of recruitment of RILP to the phagosome, tubular vesicles expressing RILP have been observed to be elongated from the MTOC, fusing with the phagosome (16). RILP has been reported to be absent from the *Mycobacterium bovis* strain BCG phagosome despite Rab7 localization (17). We have previously shown that Rab7 is transiently recruited to, and subsequently released from, *M.tb* phagosomes (4), but the interaction of RILP with *M.tb* phagosomes has not been previously reported. We examined the subcellular localization of EGFP-RILP in macrophages infected with *M.tb* (Fig. 2). In *M.tb*-infected macrophages, RILP-positive phagosomes appeared and increased to 30% of *M.tb* phagosomes up until 30 min post infection (Fig. 2a, c). No further increase was seen after this time (Fig. 2b, c). On the other hand, the proportion of RILP-positive *Staphylococcus aureus* phagosomes continued to increase beyond 30 min post infection (Fig. 2c). We also found that the proportion of RILP-positive phagosomes containing heat-inactivated *M.tb* reached more than 80% at 6 hr post infection. These results suggest that further recruitment of RILP to phagosomes containing live *M.tb* after 30 min post infection might be actively inhibited.

Next, we examined whether recruitment of CD63 and RILP to phagosomes depends on the function of Rab7 in macrophages. Raw264.7 macrophages transfected with two plasmids encoding either EGFP-fused CD63 or RILP and a dominant-negative form of Rab7, Rab7T22N, were allowed to phagocytose latex-beads for 2 hr and were then examined by CLSM for localization of lysosomal proteins on the phagosomes. Both lysosomal markers were localized to latex-bead-containing phagosomes in the control cells (Fig. 3a-1, b-1). CD63 was found on the majority of latex-bead-containing phagosomes in the cells expressing Rab7T22N (Fig. 3a-2, a-3), as well as in the control cells. However, consistent with previous findings, RILP

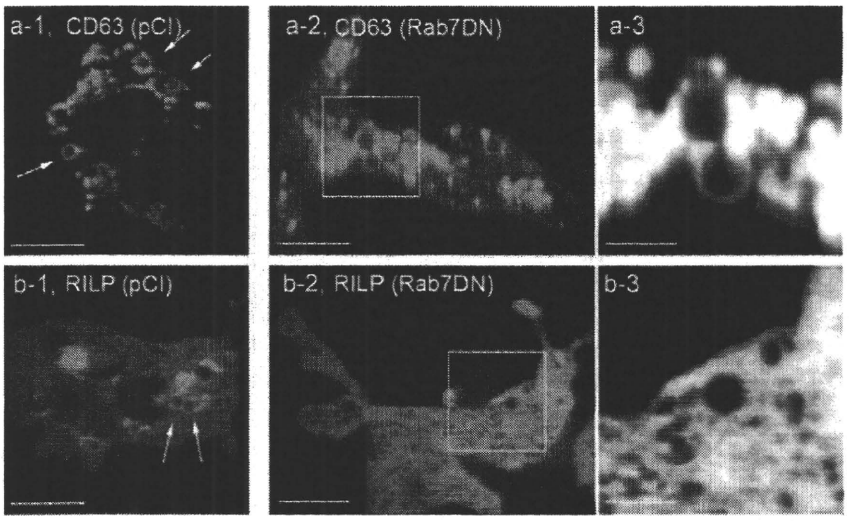

Fig. 3. Localization of lysosomal markers on latex-bead-containing phagosomes in Raw264.7 macrophages expressing dominant-negative Rab7. Raw264.7 macrophages expressing (a-2, a-3) Rab7T22N together with CD63-EGFP or (b-2, b-3) EGFP-RILP were allowed to phagocytose latex beads. Cells were fixed 2 hr after phagocytosis and observed by CLSM. (a-1, b-1) Cell images transfected with a control plasmid instead of the plasmid expressing Rab7T22N. (b-3, c-3) Enlarged images of phagosomes presented in b-2 and c-2, respectively. Scale bar, 10 μm (left and middle), 3 μm (right). pCI, cell images transfected with a control plasmid.

was not present on latex-bead phagosomes in cells expressing Rab7T22N (Fig. 3b-2, b-3) (17). We also found that clustering of RILP in the perinuclear regions was disrupted and diffused by the expression of Rab7T22N. Collectively, our data demonstrate that Rab7 is vital for recruiting RILP to phagosomes during the maturation process, but not for recruiting CD63.

How *M.tb* escapes the effects of the bactericidal components within the phagosome while still acquiring nutrients for growth is very important question. It has been suggested that mycobacterial phagosomes arrest their maturation at an early stage and completely avoid fusion with lysosomes (18, 19). However, we have shown the localization of CD63 (Fig. 2) and LAMP-2 (4) on *M.tb* phagosomes in macrophages. It has been proposed that phagolysosome biogenesis is achieved by a series of fusions with heterogeneous lysosomes (20). This model is supported by a report demonstrating the existence of subpopulations of lysosomes in macrophages (6). Our previous and current studies demonstrating the alternative localization of lysosomal markers on *M.tb* phagosomes further support this model. From these observations, it seems that dissociation of Rab7 from *M.tb* phagosomes selectively inhibits fusion with harmful lysosomes despite continued fusion with non-microbicidal lysosomes.

In conclusion, based on our findings we propose the following model for *M.tb*-induced inhibition of phagolysosome biogenesis: Early *M.tb* phagosomes are capable of recruiting Rab7 and can potentially fuse with lysosomes. RILP is also recruited to *M.tb* phagosomes, which form the Rab7-RILP-dynein/dynactin protein complex followed by promotion of phagolysosome biogenesis. However, viable *M.tb* is able to release Rab7 from phagosomes, resulting in inhibition of further fusion with lysosomal vesicles and disassembly of the RILP-phagosome complex. This causes the blocking of subsequent phagolysosome biogenesis. On the other hand, non-microbicidal vesicles expressing CD63 and/or LAMP-2 continuously fuse with *M.tb* phagosomes despite Rab7 dissociation, and this fusion would support the acquisition of nutrients for mycobacterial proliferation within the phagosome.

ACKNOWLEDGMENTS

We thank Drs. Toshi Nagata and Masato Uchijima (Hamamatsu University School of Medicine, Hamamatsu, Japan) for their helpful discussion. *M.tb* strain H37Rv was kindly provided by Dr. Isamu Sugawara (Research Institute of Tuberculosis, Tokyo, Japan). This work was supported in part by Grants-in-Aid for Scientific Research from the Japan Society for the Promotion of Science, COE Research and Scientific Research on Priority Areas from the Ministry of Education, Culture, Sports, Science and Technology

of Japan, Health and Labor Science Research Grants for Research into Emerging and Reemerging Infectious Diseases from the Ministry of Health, Labor and Welfare of Japan, and the United States-Japan Cooperative Medical Science Committee.

REFERENCES

1. Armstrong J.A., Hart P.D. (1971) Response of cultured macrophages to *Mycobacterium tuberculosis*, with observations on fusion of lysosomes with phagosomes. *J Exp Med* **134**: 713–40.
2. Clemens D.L., Horwitz M.A. (1995) Characterization of the *Mycobacterium tuberculosis* phagosome and evidence that phagosomal maturation is inhibited. *J Exp Med* **181**: 257–70.
3. Van Der Wel N., Hava D., Houben D., Fluitsma D., Van Zon M., Pierson J., Brenner M., Peters P.J. (2007) *M. tuberculosis* and *M. leprae* translocate from the phagolysosome to the cytosol in myeloid cells. *Cell* **129**: 1287–98.
4. Seto S., Matsumoto S., Ohta I., Tsujimura K., Koide Y. (2009) Dissection of Rab7 localization on *Mycobacterium tuberculosis* phagosome. *Biochem Biophys Res Commun* **387**: 272–7.
5. Aoki K., Matsumoto S., Hirayama Y., Wada T., Ozeki Y., Niki M., Domenech P., Umemori K., Yamamoto S., Mineda A., Matsumoto M., Kobayashi K. (2004) Extracellular mycobacterial DNA-binding protein 1 participates in mycobacterium-lung epithelial cell interaction through hyaluronic acid. *J Biol Chem* **279**: 39798–806.
6. Astarie-Dequeker C., Carreno S., Cougoule C., Maridonneau-Parini I. (2002) The protein tyrosine kinase Hck is located on lysosomal vesicles that are physically and functionally distinct from CD63-positive lysosomes in human macrophages. *J Cell Sci* **115**: 81–9.
7. Fratti R.A., Chua J., Deretic V. (2003) Induction of p38 mitogen-activated protein kinase reduces early endosome auto-antigen 1 (EEA1) recruitment to phagosomal membranes. *J Biol Chem* **278**: 46961–7.
8. Nieuwenhuis H.K., Van Oosterhout J.J., Rozemuller E., Van Iwaarden F., Sixma J.J. (1987) Studies with a monoclonal antibody against activated platelets: evidence that a secreted 53 000-molecular weight lysosome-like granule protein is exposed on the surface of activated platelets in the circulation. *Blood* **70**: 838–45.
9. Bampton E.T., Goemans C.G., Niranjan D., Mizushima N., Tolkovsky A.M. (2005) The dynamics of autophagy visualized in live cells: from autophagosome formation to fusion with endo/lysosomes. *Autophagy* **1**: 23–36.
10. Fukuda M. (1991) Lysosomal membrane glycoproteins: structure, biosynthesis, and intracellular trafficking. *J Biol Chem* **266**: 21327–30.
11. Metzelaar M.J., Wijngaard P.L., Peters P.J., Sixma J.J., Nieuwenhuis H.K., Clevers H.C. (1991) CD63 antigen. A novel lysosomal membrane glycoprotein cloned by a screening procedure for intracellular antigens in eukaryotic cells. *J Biol Chem* **266**: 3239–45.
12. Artavanis-Tsakonas K., Love J.C., Ploegh H.L., Vyas J.M. (2006) Recruitment of CD63 to *Cryptococcus neoformans* phagosomes requires acidification. *Proc Natl Acad Sci U S A* **103**: 15945–50.
13. Beatty W.L., Rhoades E.R., Hsu D.K., Liu F.T., Russell D.G. (2002) Association of a macrophage galactoside-binding protein with Mycobacterium-containing phagosomes. *Cell Microbiol* **4**: 167–76.
14. Cantalupo G., Alifano P., Roberti V., Bruni C.B., Bucci C. (2001) Rab-interacting lysosomal protein (RILP): the Rab7 effector required for transport to lysosomes. *Embo J* **20**: 683–93.
15. Jordens I., Fernandez-Borja M., Marsman M., Dusseljee S., Janssen L., Calafat J., Janssen H., Wubbolts R., Neefjes J. (2001) The Rab7 effector protein RILP controls lysosomal transport by inducing the recruitment of dynein-dynactin motors. *Curr Biol* **11**: 1680–5.
16. Harrison R.E., Bucci C., Vieira O.V., Schroer T.A., Grinstein S. (2003) Phagosomes fuse with late endosomes and/or lysosomes by extension of membrane protrusions along microtubules: role of Rab7 and RILP. *Mol Cell Biol* **23**: 6494–506.
17. Sun J., Deghmane A.E., Soualhine H., Hong T., Bucci C., Solodkin A., Hmama Z. (2007) *Mycobacterium bovis* BCG disrupts the interaction of Rab7 with RILP contributing to inhibition of phagosome maturation. *J Leukoc Biol* **82**: 1437–45.
18. Deretic V., Singh S., Master S., Harris J., Roberts E., Kyei G., Davis A., De Haro S., Naylor J., Lee H.H., Vergne I. (2006) *Mycobacterium tuberculosis* inhibition of phagolysosome biogenesis and autophagy as a host defence mechanism. *Cell Microbiol* **8**: 719–27.
19. Deretic V., Vergne I., Chua J., Master S., Singh S.B., Fazio J.A., Kyei G. (2004) Endosomal membrane traffic: convergence point targeted by *Mycobacterium tuberculosis* and HIV. *Cell Microbiol* **6**: 999–1009.
20. Rohde K., Yates R.M., Purdy G.E., Russell D.G. (2007) *Mycobacterium tuberculosis* and the environment within the phagosome. *Immunol Rev* **219**: 37–54.

Vaccine 28 (2010) 2026–2031

Contents lists available at ScienceDirect

Vaccine

journal homepage: www.elsevier.com/locate/vaccine

Identification of HLA-DR4-restricted T-cell epitope on MPT51 protein, a major secreted protein derived from *Mycobacterium tuberculosis* using MPT51 overlapping peptides screening and DNA vaccination

Li-Xin Wang[a], Toshi Nagata[b,*], Kunio Tsujimura[a], Masato Uchijima[a], Shintaro Seto[a], Yukio Koide[a]

[a] Department of Infectious Diseases, Hamamatsu University School of Medicine, 1-20-1 Higashi-ku, Handa-yama, Hamamatsu 431-3192, Japan
[b] Department of Health Science, Hamamatsu University School of Medicine, 1-20-1 Higashi-ku, Handa-yama, Hamamatsu 431-3192, Japan

ARTICLE INFO

Keywords:
DNA immunization
Th epitope
Mycobacterium tuberculosis

ABSTRACT

We identified a novel HLA-DR4-restricted CD4+ T-cell epitope on a secreted antigen of *Mycobacterium tuberculosis*, MPT51, in 004149-MM HLA-DR4-transgenic mice which express HLA-DRB1*0401, but not murine MHC class II molecules. The mice were immunized with plasmid DNA encoding MPT51 using gene gun and interferon (IFN)-γ production from the immune splenocytes was analyzed. In response to overlapping synthetic peptides covering the mature MPT51 sequence, only one peptide, p191–210, stimulated the splenocytes to produce IFN-γ. Further analysis using flow cytometry and computer-assisted algorithm, ProPred, narrowed down the region of CD4+ T-cell epitope to p191–202. The CD4+ T-cell epitope would be feasible for vaccine design against tuberculosis as well as for analysis of MPT51-specific T-cells in *M. tuberculosis* infection.

1. Introduction

Tuberculosis (TB) has been a major cause of illness and death worldwide. There were estimated 9.2 million new causes and 1.7 million deaths from TB in 2006 [1]. Although WHO's "The Stop TB Strategy" approach seems to work, especially in the African region, multi-drug resistant strains and co-infection with human immunodeficiency virus (HIV) remains difficult issues in TB prevention (0.7 million cases and 0.2 million deaths from TB occurred in HIV-positive people in 2006 [1]). The only TB vaccine currently available is the attenuated *Mycobacterium bovis* strain Bacillus Calmette-Guérin (BCG), the effect of which has been questioned for preventing pulmonary TB in adults [2] and also reported to wane with time since vaccination [3]. Therefore, the improved vaccine is an urgent need against TB [2,4].

It has been widely accepted that cell-mediated immunity plays a pivotal role in the control of *Mycobacterium tuberculosis* infection [5,6]. CD4+ type 1 helper T (Th1) cells are involved in the development of resistance to the disease, primarily through the production of macrophage-activating cytokines such as interferon (IFN)-γ and tumor necrosis factor-α. In addition, CD8+ cytotoxic T-lymphocytes (CTL) have also been reported to contribute to disease resistance [5,6].

Secreted and surface-exposed cell wall proteins, virulence factors such as PE/PPE and EsX have been reported to be immunodominant antigens, which are able to induce protective cellular immunity against TB [7–9]. The mouse model of TB infection revealed that memory cells from immune mice produced substantial amounts of IFN-γ in response to two fractions of culture filtrate of *M. tuberculosis* represented by 6–10 kDa proteins and antigen 85 (Ag85) complex, a 30–32 kDa protein family [7,8,10,11].

Ag85 complex (Ag85A, Ag85B, and Ag85C), which possesses mycolyltransferase activity in cell wall synthesis and in the biogenesis of cord factor [12] and has been shown to be a major fraction of the secreted proteins of *M. tuberculosis* [13]. Another major secreted protein, termed MPT51, has primary structure similarity (38–43%) with those components and the antibody (Ab) against MPT51 was demonstrated to cross-react with the three components of Ag85 complex [13,14]. Using DNA vaccine encoding MPT51, we found that MPT51 can induce specific cellular immune responses and the protective immunity against challenge with *M. tuberculosis* in murine infection model [15]. We identified murine T-cell epitopes using C57BL/6 and BALB/c mouse strains [16,17] and an HLA-A*0201-restricted CD8+ T-cell epitope in MPT51 molecule [18].

Here, we identified an HLA-DRB1*0401-restricted CD4+ T-cell epitope on MPT51 with a strategy using HLA-DRB1*0401-transgenic (Tg) mice, gene gun immunization with expression plasmid DNA encoding MPT51, overlapping synthetic peptides spanning the entire mature MPT51 amino acid (aa) sequence, and the computer-assisted major histocompatibility complex (MHC) binding peptide prediction algorithms.

* Corresponding author. Tel.: +81 53 435 2332; fax: +81 53 435 2332.
E-mail address: tnagata@hama-med.ac.jp (T. Nagata).

0264-410X/$ – see front matter © 2009 Elsevier Ltd. All rights reserved.
doi:10.1016/j.vaccine.2009.10.063

2. Materials and methods

2.1. Animals

HLA-DRB1*0401-Tg mice (004149-MM) [19] were purchased from Taconic Farms, Inc. (Hudson, NY, USA). The 004149-MM mice do not express H2 class II molecules, but express HLA-DRB1*0401 composed of *HLA-DRA-IEα* and *HLA-DRB1*0401-IEβ* chimeric genes [19]. In 004149-MM mice, the HLA-DRB1*0401 is the only species of MHC class II molecule expressed. The mice were kept under specific pathogen-free conditions and fed autoclaved food and water *ad libitum* at the Institute for Experimental Animals of the Hamamatsu University School of Medicine. Two to three-month-old female mice were used in all experiments. Animal experiments were performed according to the Guidelines for Animal Experimentation, Hamamatsu University School of Medicine.

2.2. Peptides

Peptides spanning the entire mature MPT51 aa sequence of *M. tuberculosis* (266 aa residues) were synthesized as 20-mer peptides overlapping by 10 residues, with the exception of the carboxy-terminal 12-mer from aa 255 to 266, were described in our previous work [16]. Briefly, lyophilized peptides were purchased from Invitrogen Corporation (Carlsbad, CA, USA), purity of which was confirmed by mass spectrometry. All peptides were dissolved in distilled water to a concentration of 1 mM and stored at −80 °C until use.

2.3. Immunization of mice

For DNA immunization with Helios gene gun system (Bio-Rad Laboratories, Hercules, CA, USA), preparation of DNA-coated gold particle cartridge was followed to the manufacturer's instruction manual. Finally, 0.5 mg of gold particles was coated with 2 μg of plasmid DNA and the injection was carried out with 0.5 mg gold per shot twice. Mice were injected with 4 μg of plasmid DNA four times at 1-week intervals. Mice were also immunized subcutaneously with 1×10^6 CFU of *M. bovis* BCG (Tokyo strain; Japan BCG Inc., Tokyo, Japan) twice with a 2-week interval.

2.4. Preparation of splenocyte culture supernatants and measurement of IFN-γ amounts

Spleen cells were harvested from MPT51 DNA-immune mice. Recovered cells were plated in 96-well plates at 1×10^6 cells per well in the presence or absence of 5 μM of each MPT51 peptide at 37 °C with 5% CO_2 atmosphere. Purified protein derivative (PPD; Japan BCG Inc.) (1 μg ml^{-1}) was used as a positive control. Supernatants were harvested 72 h later and stored at −20 °C until they were assayed. Concentration of IFN-γ in the culture supernatants was determined by a sandwich enzyme-linked immunosorbent assay (ELISA). The ELISA was carried out as described in our previous work [16] with some modifications. The method is as follows. The 96-well ELISA plates (EIA/RIA Plate A/2; Costar, Cambridge, MA, USA) were coated with 2 μg ml^{-1} of capture antibody (Ab) (anti-murine IFN-γ monoclonal Ab [mAb] R4-6A2; BD Biosciences, San Jose, CA, USA) at 4 °C overnight, washed with PBS supplemented with 0.05% Tween 20 (PBS-Tween), and blocked with Block One Blocking solution (Nacalai Tesque, Kyoto, Japan) at room temperature for 45 min. After washed with PBS-Tween, the culture supernatants were added to the plates and the plates were incubated at 4 °C overnight. After washed with PBS-Tween, 0.5 μg ml^{-1} of biotin-labeled anti-murine IFN-γ mAb XMG1.2 (BD Biosciences) was added to the plates, and the plates were incubated for 2 h at room temperature. After washed with PBS-Tween, horseradish peroxidase (HRP)-conjugated avidin (Bio-Rad Laboratories) was added and incubated for 30 min at room temperature. After washed, the plates were added with TMB one component HRP microwell substrate (BioFX Laboratories, Owings Mills, MD, USA). After 10 min, the enzyme reaction was stopped by adding 2 M H_2SO_4, followed by measuring the absorbance at 450 nm using an EZS-ABS Microplate Reader (Asahi Techno Glass Tokyo, Japan).

2.5. Computer-assisted algorithms for prediction of Th epitope

Th epitope prediction of MPT51 was performed using ProPred HLA-DR binding peptide prediction algorithm ([20], http://www.imtech.res.in/raghava/propred/) at the default setting (threshold value of 3.0). This server has been used for searching the promiscuous binding regions which bind to a total of 50 alleles of HLA-DR molecules. The annotated 50 alleles are composed of 9 serologically defined HLA-DR molecules, namely, HLA-DR1 (2 alleles), DR3 (7 alleles), DR4 (8 alleles), DR7 (2 alleles), DR8 (6 alleles), DR11 (9 alleles), DR13 (11 alleles), DR15 (3 alleles) and DR51 (2 alleles). In addition, RANKPEP MHC binding peptide prediction algorithm ([21], http://immunax.dfci.harvard.edu/Tools/rankpep.html) was also used in this study.

2.6. Intracellular IFN-γ staining

Antigen-specific T-cell subset was also determined with simultaneous flow cytometric assessment of T-cell phenotype and intracellular IFN-γ synthesis. Cell-surface staining of CD4 and CD8 and intracellular IFN-γ staining were described in our previous work [16,17]. Intracellular IFN-γ staining was conducted using a Cytofix/Cytoperm Plus (with GolgiStop) kit (BD Biosciences) according to the manufacturer's instruction.

2.7. Statistics

Statistical analyses were performed by using StatView-J 5.0 statistics program (Abacus Concepts, Berkeley, CA, USA). Data were analyzed with unpaired Student's *t* test.

3. Results

3.1. IFN-γ production in response to overlapping synthetic peptides from MPT51 by splenocytes of pCI-MPT51 DNA or M. bovis BCG-immune 004149-MM HLA-DRB1*0401-Tg mice

The 004149-MM mice do not express H2 class II molecules, but express HLA-DR4 transgene [19]. Expression of HLA-DR molecules on splenocytes of the mice was confirmed by flow cytometric analysis with anti-HLA DR mAb (data not shown). Splenocytes from 004149-MM HLA-DRB1*0401-Tg mice immunized with plasmid DNA encoding mature MPT51 (pCI-MPT51) were stimulated with the overlapping MPT51 peptides for 72 h and IFN-γ concentration of culture supernatants was measured by ELISA. As shown in Fig. 1, robust IFN-γ production was observed in the splenocytes only in the presence of peptide 191 (p191; aa 191–210). As expected, splenocytes from naïve 004149-MM mice showed no significant IFN-γ production in response to any MPT51 peptides. In addition, we examined the dose–response relationship by adding serial amounts of MPT51 p191 peptide to the splenocyte culture. The minimal concentration of the peptide for inducing IFN-γ production by the splenocytes was approximately 1×10^{-8} M (10 nM) (data not shown).

In order to examine whether the same peptide induce IFN-γ following natural mycobacterial infection, splenocytes from 004149-MM HLA-DRB1*0401-Tg mice immunized with *M. bovis* BCG were examined for IFN-γ production in response to MPT51

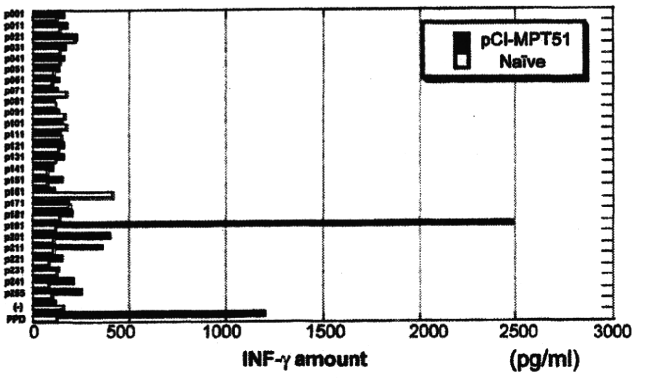

Fig. 1. IFN-γ production of spleen cells from 004149-MM HLA-DRB1*0401-Tg mice immunized with pCI-MPT51. IFN-γ production of splenocytes from the mice immunized with pCI-MPT51 plasmid in response to 1 of 26 overlapping peptides (5 μM) covering MPT51 molecule, medium alone [(−)], or PPD (1 μg ml^{-1}) was evaluated. The splenocytes from naïve mice were also examined as a control. Data are representatives of three independent experiments.

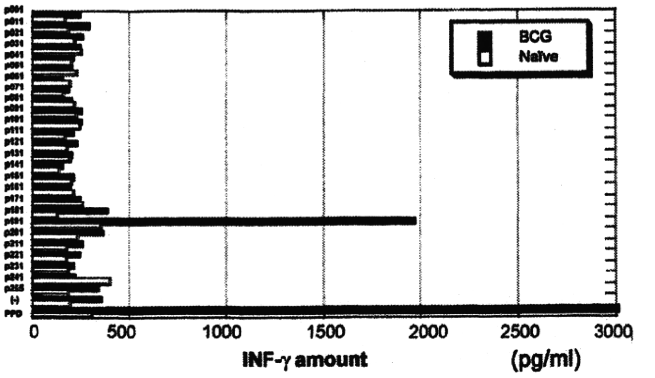

Fig. 2. IFN-γ production of spleen cells from 004149-MM HLA-DRB1*0401-Tg mice immunized with *M. bovis* BCG. IFN-γ production of splenocytes from the mice immunized with *M. bovis* BCG in response to 1 of 26 overlapping peptides (5 μM) covering MPT51 molecule, medium alone [(−)], or PPD (1 μg ml^{-1}) was evaluated. The splenocytes from naïve mice were also examined as a control. Data are representatives of three independent experiments.

peptides. Robust production of IFN-γ was observed in the presence of PPD (Fig. 2). Only MPT51 p191 among all MPT51 peptides induced production of high amounts of IFN-γ similarly to the case of MPT51 DNA-immunized mice.

3.2. Prediction of CD4+ T-cell epitope on peptide 191 of MPT51

We predicted CD4+ T-cell epitope candidate peptides in the 20-mer peptide by computer-based program, ProPred [20]. We found that a core HLA-DRB1*0401 binding motif composed of 9-mer peptide, p194–202 (WVWSPTNPG) at the default threshold setting. This amino acid region was also predicted to bind to HLA-DR4 at the highest score (17.65) in RANKPEP algorithm [21]. This core region (p194–202) was predicted to bind 20 alleles from a total of 50 alleles listed in ProPred program (Fig. 3). These HLA-DR alleles include 6 alleles in HLA-DR3 serological group, 8 alleles in HLA-DR4 group, 2 alleles in HLA-DR7 group, 2 alleles in HLA-DR11 group, and 2 alleles in HLA-DR13 group. Thus, the region (p194–202) was predicted to bind 40% HLA-DR alleles included in the ProPred program. In general, 12–20-mer antigenic peptides bind to MHC class II molecules. Therefore, we synthesized p191–202 peptide as a candidate CD4+ T-cell epitope, instead of examining jus t a core motif (p194–202) for the following experiment.

3.3. Detection of MPT51 p191–202-, or p191–210-specific CD4+ T-cells in 004149-MM HLA-DRB1*0401-Tg mice by ELISA and intracellular IFN-γ staining

We then examined splenocytes derived from MPT51 DNA-immune 004149-MM HLA-DRB1*0401-Tg mice for detection of

```
                171        181        191        201        211        220
                LGRWKWHDPWVHASLLAQNNTRVWVWSPTNPGASDPAAMIGQAAEAMGNS

DRB1*0401       LGRWKWHDPWVHASLLAQNNTRVWVWSPTNPGASDPAAMIGQAAEAMGNS
DRB1*0404       LGRWKWHDPWVHASLLAQNNTRVWVWSPTNPGASDPAAMIGQAAEAMGNS
DRB1*0405       LGRWKWHDPWVHASLLAQNNTRVWVWSPTNPGASDPAAMIGQAAEAMGNS
DRB1*0408       LGRWKWHDPWVHASLLAQNNTRVWVWSPTNPGASDPAAMIGQAAEAMGNS
DRB1*0410       LGRWKWHDPWVHASLLAQNNTRVWVWSPTNPGASDPAAMIGQAAEAMGNS
DRB1*0421       LGRWKWHDPWVHASLLAQNNTRVWVWSPTNPGASDPAAMIGQAAEAMGNS
DRB1*0423       LGRWKWHDPWVHASLLAQNNTRVWVWSPTNPGASDPAAMIGQAAEAMGNS
DRB1*0426       LGRWKWHDPWVHASLLAQNNTRVWVWSPTNPGASDPAAMIGQAAEAMGNS

DRB1*0305       LGRWKWHDPWVHASLLAQNNTRVWVWSPTNPGASDPAAMIGQAAEAMGNS
DRB1*0306       LGRWKWHDPWVHASLLAQNNTRVWVWSPTNPGASDPAAMIGQAAEAMGNS
DRB1*0307       LGRWKWHDPWVHASLLAQNNTRVWVWSPTNPGASDPAAMIGQAAEAMGNS
DRB1*0308       LGRWKWHDPWVHASLLAQNNTRVWVWSPTNPGASDPAAMIGQAAEAMGNS
DRB1*0309       LGRWKWHDPWVHASLLAQNNTRVWVWSPTNPGASDPAAMIGQAAEAMGNS
DRB1*0311       LGRWKWHDPWVHASLLAQNNTRVWVWSPTNPGASDPAAMIGQAAEAMGNS

DRB1*0701       LGRWKWHDPWVHASLLAQNNTRVWVWSPTNPGASDPAAMIGQAAEAMGNS
DRB1*0703       LGRWKWHDPWVHASLLAQNNTRVWVWSPTNPGASDPAAMIGQAAEAMGNS

DRB1*1114       LGRWKWHDPWVHASLLAQNNTRVWVWSPTNPGASDPAAMIGQAAEAMGNS
DRB1*1120       LGRWKWHDPWVHASLLAQNNTRVWVWSPTNPGASDPAAMIGQAAEAMGNS

DRB1*1302       LGRWKWHDPWVHASLLAQNNTRVWVWSPTNPGASDPAAMIGQAAEAMGNS
DRB1*1323       LGRWKWHDPWVHASLLAQNNTRVWVWSPTNPGASDPAAMIGQAAEAMGNS
```

Fig. 3. Prediction of HLA-DR binding sites in MPT51 protein. Prediction of HLA-DR binding sites of MPT51 was performed with ProPred algorithm. The 20 HLA-DR alleles on which MPT51 p194–202 is predicted to be a core binding motif, are shown. Bold letters indicate predicted binding sites of MPT51 for each HLA-DR allele.

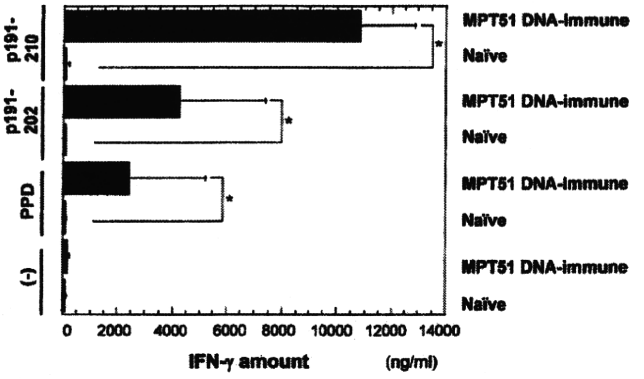

Fig. 4. IFN-γ production of MPT51 DNA-immune 004149-MM HLA-DRB1*0401-Tg mice splenocytes in response to MPT51 p191–210 or p191–202 peptides. IFN-γ production from splenocytes of MPT51 DNA-immune or naïve 004149-MM HLA-DRB1*0401-Tg mice was analyzed in the presence of MPT51 p191–210 (20-mer) or p191–202 (12-mer) peptides. Data are means and standard deviations from five to eight experiments. Asterisk indicates statistically significance with Student's *t* test ($p < 0.05$).

MPT51 p191–202-, or p191–210-specific T-cells. As shown in Fig. 4, the immune splenocytes, but not naïve splenocytes produced robust amounts of IFN-γ in response to MPT51 p191–202, suggesting that MPT51 p191–202 peptide is a *bona fide* HLA-DRB1*0401-restricted CD4+ T-cell epitope. Further, we examined whether CD4+ T-cells produce IFN-γ in response to MPT51 p191–202 or p191–210 peptide with intracellular IFN-γ staining assay. Again, MPT51 DNA-immune, but not naïve CD4+ T-cells produced IFN-γ in response to these MPT51 peptides (Fig. 5).

4. Discussion

Understanding of the nature of protective immunity to *M. tuberculosis* would facilitate the development of the future vaccine. The cellular arm of the immune response mediated by CD4+ Th1 cells and CD8+ CTL has been established as a pivotal component of the protective immunity against *M. tuberculosis* [5,6]. CD4+ Th1 cells have been reported to contribute to protection against *M. tuberculosis* infection through inflammatory cytokine production such as IFN-γ. IFN-γ has been considered to contribute to the protective immunity through activating macrophages and increasing natural killer cell activity. However, IFN-γ production has been shown not to be the only correlate of protection against *M. tuberculosis* [22]. Production of IL-2 [23,24] or functions such as direct cytotoxic ability of CD4+ T-cells [25,26] may be important for the protective ability. Functions of MPT51 p191–202-specific CD4+ T-cells in this report except for IFN-γ production should be clarified in further study.

Reports concerning the involvement of CD4+ T-cells to contain *M. tuberculosis* infection have accumulated and an intense effort to identify *M. tuberculosis*-derived CD4+ T-cell epitopes that are presented by HLA class II molecules, has been done. HLA-DR-restricted T-cell epitopes in *M. tuberculosis* antigens have been identified, including epitopes in heat shock protein 65 [27], Ag 85B [28], ESAT-6 [29], Mce proteins [30], MPB70 [31], the 24 kDa secreted lipoprotein (LppX) [32], and PPE68 [33]. MPT51 is a dominant *M. tuberculosis*-derived secreted molecule which is related with Ag85 family molecules, Ag85A, Ag85B, and Ag85C. The molecules have been reported in a variety of mycobacteria. Functionally, the molecule has been implicated in fibronectin binding as in Ag85 family molecules [34]. However, MPT51 appears not to have mycolyltransferase activity that Ag85 family molecules share since MPT51 does not conserve the catalytic triad (Ser-His-Glu) in the aa sequence [35]. Therefore, MPT51 seems to have the particular function that remains to be clarified. Importantly, MPT51 has been reported as a potential marker for the diagnosis of TB, especially in AIDS patients. Ramalingam et al. [36] reported that early immune responses against 38 kDa and 27 kDa (MPT51) proteins were detected in pulmonary TB accompanied with HIV infection. In addition, we demonstrated that MPT51 plays a pivotal role in the protection against *M. tuberculosis* infection [15]. The identification of human T-cell epitopes in MPT51 protein would be very useful for early diagnosis of TB and development of TB vaccine.

HLA-Tg mice have been widely used for detection of HLA class II-restricted T-cell epitopes [37,38]. We used in this study 004149-MM HLA-DRB1*0401-Tg mice [19]. The Tg mice express the transgene-encoded proteins consisted of antigen-binding domains from HLA-DRA and HLA-DRB1*0401 molecules and the remaining domains from the H2-E^d-α and H2-E^d-β chains, which has the same antigen-binding specificity as HLA-DRB1*0401 molecules and function of presenting antigens to T-cells. In addition, the molecules are the only species of MHC class II molecule expressed in the mice due to endogenous H2-Aβ, H2-Eα deficiency [19].

We predicted HLA-DR-restricted T-cell epitope candidates in the 20-mer peptide by computer-based program, ProPred [20] in this study. The ProPred algorithm is a virtual matrix-based T-cell epitope prediction program based on TEPITOPE program [39]. TEPITOPE first extracts all possible 9-amino acid peptide frames from

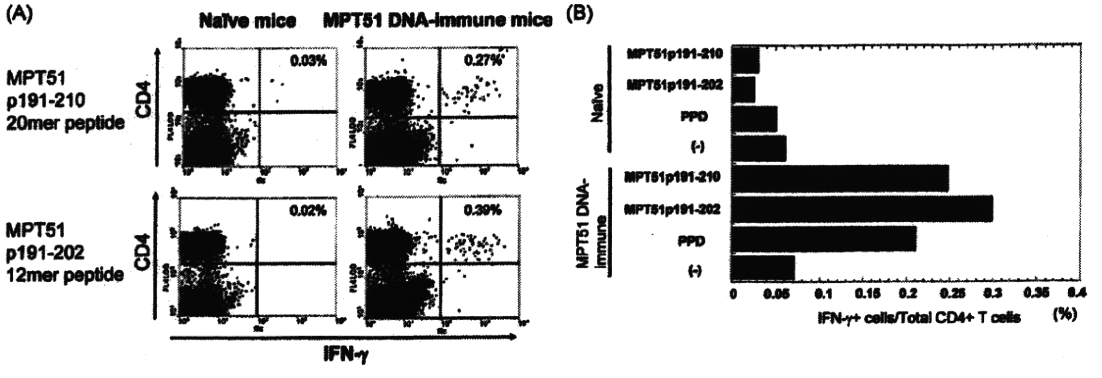

Fig. 5. Intracellular IFN-γ staining of spleen cells from MPT51 DNA-immune 004149-MM HLA-DRB1*0401-Tg mice. (A) The graph shows the percentages of IFN-γ-producing cells in total CD4+ T-cells after 4 h of stimulation with MPT51 p191–210 or p191–202 peptides. Intracellular IFN-γ and CD4 were detected by flow cytometry in or on the immune spleen cells after in vitro stimulation with the peptides. There were, however, no intracellular IFN-γ-positive CD8+ T-cells after in vitro stimulation with these peptides (data not shown). (B) Summary of frequency of IFN-γ-producing cells in CD4+ T-cells in spleens of MPT51 DNA-immune 004149-MM HLA-DRB1*0401-Tg mice. Data are means from two to four experiments.

the input protein sequence. Each amino acid in this 9-mer peptide is assigned to relative binding values using the position-specific, and peptide side chain-specific values from the virtual matrices. The first anchor position (p1) was shown to be a key factor for high affinity binding to HLA-DR molecules and only aliphatic or aromatic amino acid residues are considered as p1 anchor [40,41]. We found a core HLA-DRB1*0401 binding motif composed of 9-mer peptide, p194–202 (WVWSPTNPG) in MPT51 p191–210 region at the default threshold setting of ProPred algorithm. As described in Section 3, the same region was also predicted to bind to HLA-DR4 at the highest score in RANKPEP algorithm [21], which is programmed on position-specific scoring matrices.

MHC class II binding motifs are not so restricted compared with MHC class I binding motifs, but some rules of MHC class II binding motifs have been reported. The DRB1*0401 binding motif was reported to require an aromatic or aliphatic anchor residue in position 1 (Y, W, F, L, I, V, M), and another anchor residue in position 6, defined as either a hydroxyl (S or T) or hydrophobic (L, V, I, or M) residue [42]. MPT51 p194–202 amino acid residues, W in position 1 and T in position 6, fit the rule.

T-cell epitopes which are restricted to a variety of HLA alleles (promiscuous T-cell epitopes) are quite useful for development of epitope vaccines and diagnostic tools as human population is heterogeneous for HLA alleles. As described in Section 3, this region was predicted to bind 20 alleles among a total of 50 alleles of HLA-DR type in ProPred algorithm (40%). This result suggests that the region is a promiscuous T-cell epitope, although a report mentioned that the peptides predicted to bind over 50% HLA-DR alleles in ProPred were considered promiscuous for binding [43]. The frequency of the memory T-cells and the kinetics in human subjects after *M. tuberculosis* infection would be important issues to be clarified in future.

In conclusion, we identified one HLA-DRB1*0401-restricted CD4+ Th1 epitope on MPT51 in HLA-DRB1*0401-Tg mice, which may play a pivotal role in the protection against *M. tuberculosis* infection. The identification of these T-cell epitopes will be very useful for further elucidation of the role of MPT51-specific T-cells in the protective immunity and also for future TB vaccine design.

Acknowledgements

This work was supported by grants-in-aid for scientific research from the Japanese Society for the Promotion of Science (grant 20590438 to T. N. and grant 20390125 to Y. K.), by a grant-in-aid for the Centers of Excellence (COE) Research Program from the Ministry of Education, Culture, Sports, Science and Technology of Japan, and by a grant-in-aid from the United States-Japan Cooperative Medical Science Program.

References

[1] World Health Organization. WHO Report 2007 Global tuberculosis control: surveillance, planning, financing. Geneva; 2008 [online]. http://www.who.intentity/tb/publications/global_report/2008/pdf/fullreport.pdf.
[2] Andersen P, Doherty TM. The success and failure of BCG—implications for a novel tuberculosis vaccine. Nature Rev Microbiol 2005;3:656–62.
[3] Sterne JAC, Rodrigues LC, Guedes IN. Does the efficacy of BCG decline with time since vaccination? Int J Tuberc Lung Dis 1998;2:200–7.
[4] Kaufmann SHE. Is the development of a new tuberculosis vaccine possible? Nat Med 2000;6:955–60.
[5] Flynn JL, Chan J. Immunology of tuberculosis. Annu Rev Immunol 2001;19:93–129.
[6] Kaufmann SHE. Immunity to intracellular bacteria. In: Paul WE, editor. Fundamental immunology. 5th ed. Philadelphia: Lippincott Williams & Wilkins Publishers; 2003. p. 1229–61.
[7] Sable SB, Kalra M, Verma I, Khuller GK. Tuberculosis subunit vaccine design: the conflict of antigenicity and immunogenicity. Clin Immunol 2007;122:239–51.
[8] Andersen P, Doherty TM. TB subunit vaccines—putting the pieces together. Microbes Infect 2005;7:911–21.
[9] Bertholet S, Ireton GC, Kahn M, et al. Identification of human T cell antigens for the development of vaccines against *Mycobacterium tuberculosis*. J Immunol 2008;181:7948–57.
[10] Andersen P. Effective vaccination of mice against *Mycobacterium tuberculosis* infection with a soluble mixture of secreted mycobacterial proteins. Infect Immun 1994;62:2536–44.
[11] Andersen P, Andersen ÅB, Sørensen AL, Nagai S. Recall of long-lived immunity to *Mycobacterium tuberculosis* infection in mice. J Immunol 1995;154:3359–72.
[12] Belisle JT, Vissa VD, Sievert T, Takayama K, Brennan PJ, Besra GS. Role of the major antigen of *Mycobacterium tuberculosis* in cell wall biogenesis. Science 1997;276:1420–2.
[13] Wiker HG, Harboe M. The antigen 85 complex: a major secretion product of *Mycobacterium tuberculosis*. Microbiol Rev 1992;56:648–61.
[14] Ohara N, Kitaura H, Hotokezaka H, Nishiyama T, Wada N, Matsumoto S, et al. Characterization of the gene encoding the MPB51, one of the major secreted protein antigens of *Mycobacterium bovis* BCG, and identification of the secreted protein closely related to the fibronectin binding 85 complex. Scand J Immunol 1995;41:433–42.
[15] Miki K, Nagata T, Tanaka T, Kim Y-H, Uchijima M, Ohara N, et al. Induction of protective cellular immunity against *Mycobacterium tuberculosis* by recombinant attenuated self-destructing *Listeria monocytogenes* strains harboring eukaryotic expression plasmids for antigen 85 complex and MPB/MPT51. Infect Immun 2004;72:2014–21.
[16] Suzuki M, Aoshi T, Nagata T, Koide Y. Identification of murine H2-D^d- and H2-A^b-restricted T-cell epitopes on a novel protective antigen, MPT51, of *Mycobacterium tuberculosis*. Infect Immun 2004;72:3829–37.
[17] Aoshi T, Suzuki M, Uchijima M, Nagata T, Koide Y. Expression mapping using a retroviral vector for $CD8^+$ T cell epitopes: definition of a *Mycobacterium tuberculosis* peptide presented by H2-D^d. J Immunol Methods 2005;298:21–34.
[18] Aoshi T, Nagata T, Suzuki M, Uchijima M, Hashimoto D, Rafiei A, et al. Identification of an HLA-A*0201-restricted T-cell epitope on MPT51 protein, a major secreted protein derived from *Mycobacterium tuberculosis* by MPT51 overlapping peptide screening. Infect Immun 2008;76:1565–71.
[19] Ito K, Bian H-J, Molina M, Han J, Magram J, Saar E, et al. HLA-DR4-IE chimeric class II transgenic, murine class II-deficient mice are susceptible to experimental allergic encephalomyelitis. J Exp Med 1996;183:2635–44.
[20] Singh H, Raghava GPS. ProPred: prediction of HLA-DR binding sites. Bioinformatics 2001;17:1236–7.
[21] Reche PA, Glutting J-P, Zhang H, Reinherz EL. Enhancement to the RANKPEP resource for the prediction of peptide binding to MHC molecules using profiles. Immunogenetics 2004;56:405–19.
[22] Mittrücker H-W, Steinhoff U, Köhler A, Krause M, Lazar D, Mex P, et al. Poor correlation between BCG vaccination-induced T cell responses and protection against tuberculosis. Proc Natl Acad Sci USA 2007;104:12434–9.
[23] Millington KA, Innes JA, Hackforth S, Hinks TSC, Deeks JJ, Dosanjh DPS, et al. Dynamic relationship between IFN-γ and IL-2 profile of *Mycobacterium tuberculosis*-specific T cells and antigen load. J Immunol 2007;178:5217–26.
[24] Darrah PA, Patel DT, De Luca PM, Lindsay RWB, Davey DF, Flynn BJ, et al. Multifunctional T_H1 cells define a correlate of vaccine-mediated protection against *Leishmania major*. Nat Med 2007;13:843–50.
[25] Canady DH, Wilkinson RJ, Li Q, Harding CV, Silver RF, Boom WH. $CD4^+$ and $CD8^+$ T cells kill intracellular *Mycobacterium tuberculosis* by a perforin and Fas/Fas ligand-independent mechanism. J Immunol 2001;167:2734–42.
[26] Klucar P, Barnes PF, Kong Y, Samten B, Tvinnereim A, Spallek R, et al. Characterization of effector functions of human peptide-specific CD4+ T-cell clones for an intracellular pathogen. Human Immunol 2008;69:475–83.
[27] Mustafa AS, Lundin KA, Meloen RH, Shinnick TM, Oftung F. Identification of promiscuous epitopes from the mycobacterial 65-kilodalton heat shock protein recognized by human $CD4^+$ T cells of the *Mycobacterium leprae* memory repertoire. Infect Immun 1999;67:5683–9.
[28] Mustafa AS, Shaban FA, Abal AT, Al-Attiyah R, Wiker HG, Lundin KEA, et al. Identification and HLA restriction of naturally derived Th1-cell epitopes from the secreted *Mycobacterium tuberculosis* antigen 85B recognized by antigen-specific human $CD4^+$ T-cell lines. Infect Immun 2000;68:3933–40.
[29] Mustafa AS, Oftung F, Amoudy HA, Madi NM, Abal AT, Shaban F, et al. Multiple epitopes from the *Mycobacterium tuberculosis* ESAT-6 antigen are recognized by antigen-specific human T cell lines. Clin Infect Dis 2000;30(Suppl. 3):S201–5.
[30] Panigada M, Sturniolo T, Besozzi G, Boccieri MG, Sinigaglia F, Grassi GG, et al. Identification of a promiscuous T-cell epitope in *Mycobacterium tuberculosis* Mce proteins. Infect Immun 2002;70:79–85.
[31] Al-Attiyah R, Shaban FA, Wiker HG, Oftung F, Mustafa AS. Synthetic peptides identify promiscuous human Th1 cell epitopes of the secreted mycobacterial antigen MPB70. Infect Immun 2003;71:1953–60.
[32] Al-Attiyah R, Mustafa AS. Computer-assisted prediction of HLA-DR binding and experimental analysis for human promiscuous Th1-cell peptides in the 24 kDa secreted lipoprotein (LppX) of *Mycobacterium tuberculosis*. Scand J Immunol 2004;59:16–24.
[33] Mustafa AS, Al-Attiyah R, Hanif SNM, Shaban FA. Efficient testing of large pools of *Mycobacterium tuberculosis* RD1 peptides and identification of major antigens and immunodominant peptides recognized by human Th1 cells. Clin Vaccine Immunol 2008;15:916–24.
[34] Abou-Zeid C, Ratliff TL, Wiker HG, Harboe M, Bennedsen J, Rook GAW. Characterization of fibronectin-binding antigens released by *Mycobacterium tuberculosis* and *Mycobacterium bovis* BCG. Infect Immun 1988;56:3046–51.

[35] Wilson RA, Maughan WN, Kremer L, Besra GS, Fütterer K. The structure of *Mycobacterium tuberculosis* MPT51 (FbpC1) defines a new family of non-catalytic α/β hydrolases. J Mol Biol 2004;335:519–30.
[36] Ramalingam B, Uma Devi KR, Raja A. Isotype-specific anti-38 and 27 kDa (mpt51) response in pulmonary tuberculosis with human immunodeficiency virus coinfection. Scand J Infect Dis 2003;35:234–9.
[37] Patel SD, Cope AP, Congia M, Chen TT, Kim E, Fugger L, et al. Identification of immunodominant T cell epitopes of human glutamic acid decarboxylase 65 by using HLA-DR (α1*0101, β1*0401) transgenic mice. Proc Natl Acad Sci USA 1997;94:8082–7.
[38] Geluk A, Taneja V, van Meijgaarden KE, Zanelli E, Abou-Zeid C, Thole JE, et al. Identification of HLA class II-restricted determinants of *Mycobacterium tuberculosis*-derived proteins by using HLA-transgenic, class II-deficient mice. Proc Natl Acad Sci USA 1998;95:10797–802.
[39] Bian H, Hammer J. Discovery of promiscuous HLA-II-restricted T cell epitopes with TEPITOPE. Methods 2004;34:468–75.
[40] Hammer J, Belunis C, Bolin D, Papadopoulos J, Walsky R, Higelin J, et al. High-affinity binding of short peptides to major histocompatibility complex class II molecules by anchor combinations. Proc Natl Acad Sci USA 1994;91:4456–60.
[41] Hammer J, Bono E, Gallazzi F, Belunis C, Nagy Z, Sinigaglia F. Precise prediction of major histocompatibility complex class II-peptide interaction based on peptide side chain scanning. J Exp Med 1994;180:2353–8.
[42] Sette A, Sidney J, Oseroff C, del Guercio MF, Southwood S, Arrhenius T, et al. HLA DR4w4-binding motifs illustrate the biochemical basis of degeneracy and specificity in peptide-DR interactions. J Immunol 1993;151:3163–70.
[43] Mustafa AS, Shaban FA. ProPred analysis and experimental evaluation of promiscuous T-cell epitopes of three major secreted antigens of *Mycobacterium tuberculosis*. Tuberculosis 2006;86:115–24.

Vaccine 28 (2010) 2020–2025

Contents lists available at ScienceDirect

Vaccine

journal homepage: www.elsevier.com/locate/vaccine

Characterization of murine T-cell epitopes on mycobacterial DNA-binding protein 1 (MDP1) using DNA vaccination

Daisuke Suzuki[a,*], Toshi Nagata[b], Ghada Eweda[c], Sohkichi Matsumoto[d], Makoto Matsumoto[e], Kunio Tsujimura[c], Yukio Koide[c]

[a] 3rd Department of Internal Medicine, Hamamatsu University School of Medicine, 1-20-1 Higashi-ku, Handa-yama, Hamamatsu, Japan
[b] Department of Health Science, Hamamatsu University School of Medicine, 1-20-1 Higashi-ku, Handa-yama, Hamamatsu, Japan
[c] Department of Infectious Diseases, Hamamatsu University School of Medicine, 1-20-1 Higashi-ku, Handa-yama, Hamamatsu, Japan
[d] Department of Host Defense, Osaka City University Graduate School of Medicine, Osaka, Japan
[e] Otsuka Pharmaceutical Co., Ltd., Kagasuno 463-10 Kawauchi-cho, Tokushima, Japan

ARTICLE INFO

Keywords:
DNA immunization
T-cell epitope
Mycobacterium tuberculosis

ABSTRACT

Mycobacterial DNA-binding protein 1 (MDP1) is a major protein antigen in mycobacteria and induces protective immunity against *Mycobacterium tuberculosis* infection in mice. In this study we determined murine T-cell epitopes on MDP1 with MDP1 DNA immunization in mice. We analyzed interferon-γ production from the MDP1 DNA-immune splenocytes in response to 20-mer overlapping peptides covering MDP1 protein. We identified several CD4+ T-cell epitopes in three inbred mouse strains and one CD8+ T-cell epitope in C57BL/6 mice. These T-cell epitopes would be feasible for analysis of the role of MDP1-specific T-cells in protective immunity and for future vaccine design against *M. tuberculosis* infection.

1. Introduction

Tuberculosis (TB) has been one of the most serious infectious diseases in the world. There were estimated 9.2 million new causes and 1.7 million deaths from TB in 2006 [1]. One third of people in the world have been infected with *Mycobacterium tuberculosis* (Mtb), the causative agent of TB. Multidrug-resistant TB and co-infection of Mtb with human immunodeficiency virus are recent problems [1].

The only TB vaccine currently available is the attenuated *Mycobacterium bovis* strain Bacillus Calmette-Guérin (BCG). Although the BCG vaccine is the oldest and the most widely used vaccine [2], the effect of which has been questioned for preventing pulmonary TB in adults [3] and also to wane with time since vaccination [4]. Therefore, the improved vaccine is an urgent need against TB [5].

Cell-mediated immunity plays a pivotal role in the control of Mtb infection [6,7]. There is mounting evidence that CD4+ type 1 helper T (Th1) cells are involved in the development of resistance to the disease, primarily through the production of macrophage-activating cytokines such as interferon (IFN)-γ and tumor necrosis factor (TNF)-α. In addition, CD8+ cytotoxic T lymphocytes (CTL) contribute to disease resistance since susceptibility to Mtb is increased in mice with deficient in CD8+ T-cells [8].

Identification of protective antigens is a crucial step to develop effective vaccines against TB. Many protective antigen candidates have been reported. They include, secreted and membrane-bound proteins, virulence factors such as PE/PPE or EsX, or proteins expressed in host macrophages [9,10]. Since Mtb causes both acute disease and asymptomatic latent infection, antigens expressed in the dormant state have been also focused as target antigens for therapeutic vaccination of latent tuberculosis. Persisting bacilli resides within the hypoxic environment of the lung granulomas. Therefore, it is generally accepted that low-oxygen tension induces dormancy program of Mtb. Proteins expressed at the dormant stage include, two-component response regulator, dormancy survival regulator (*DosR*; Rv3133c) [11] and at least 20 other proteins encoded by the *DosR* regulon [12].

MDP1 is a major cellular protein of slow growers of mycobacteria [13]. The cellular content of MDP1 in mycobacterial cells increases at stationary and low-oxygen tension-induced non-replicating dormant phases [14]. MDP1 is a histone-like DNA-binding protein binding to GC-rich DNA and considered to control gene expression in mycobacteria [13,15]. MDP1 has an activity to suppress the growth rate of bacteria presumably by inhibiting macromolecular biosyntheses [16]. Recently, Lewin et al. [17] showed that reduction of MDP1 expression by antisense plasmid increased the growth of BCG in both broth culture and macrophages. They showed that the antisense DNA inhibited the

* Corresponding author. Tel.: +81 53 435 2335; fax: +81 53 435 2335.
E-mail address: zonxs@hama-med.ac.jp (D. Suzuki).

0264-410X/$ – see front matter © 2009 Elsevier Ltd. All rights reserved.
doi:10.1016/j.vaccine.2009.10.062